

## Search for Strange Pentaquark Production in $e^+e^-$ Annihilations at $\sqrt{s} = 10.58$ GeV and in $\Upsilon(4S)$ Decays

The *BABAR* Collaboration

October 20, 2004

### Abstract

We present a preliminary inclusive search for strange pentaquark production in  $e^+e^-$  interactions at a center-of-mass energy of 10.58 GeV using  $123 \text{ fb}^{-1}$  of data collected with the *BABAR* detector. We look for the states that have been reported previously: the  $\Theta^+(1540)$ , interpreted as a  $udud\bar{s}$  state; and the  $\Xi^{--}(1860)$  and  $\Xi^0(1860)$ , candidate  $dsds\bar{u}$  and  $uss(u\bar{u} + d\bar{d})$  states, respectively. In addition we search for other members of the antidecuplet and corresponding octet to which these states are thought to belong. We find no evidence for the production of such states and set preliminary limits on their production cross sections as functions of c.m. momentum. The corresponding limits on the  $\Theta^+(1540)$  and  $\Xi^{--}(1860)$  rates per  $e^+e^- \rightarrow q\bar{q}$  event are well below the rates measured for ordinary baryons of similar mass.

Submitted to the 32<sup>nd</sup> International Conference on High-Energy Physics, ICHEP 04,  
16 August—22 August 2004, Beijing, China

*Stanford Linear Accelerator Center, Stanford University, Stanford, CA 94309*

---

Work supported in part by Department of Energy contract DE-AC03-76SF00515.

The BABAR Collaboration,

B. Aubert, R. Barate, D. Boutigny, F. Couderc, J.-M. Gaillard, A. Hicheur, Y. Karyotakis, J. P. Lees,  
V. Tisserand, A. Zghiche

*Laboratoire de Physique des Particules, F-74941 Annecy-le-Vieux, France*

A. Palano, A. Pompili

*Università di Bari, Dipartimento di Fisica and INFN, I-70126 Bari, Italy*

J. C. Chen, N. D. Qi, G. Rong, P. Wang, Y. S. Zhu

*Institute of High Energy Physics, Beijing 100039, China*

G. Eigen, I. Ofte, B. Stugu

*University of Bergen, Inst. of Physics, N-5007 Bergen, Norway*

G. S. Abrams, A. W. Borgland, A. B. Breon, D. N. Brown, J. Button-Shafer, R. N. Cahn, E. Charles,  
C. T. Day, M. S. Gill, A. V. Gritsan, Y. Groysman, R. G. Jacobsen, R. W. Kadel, J. Kadyk, L. T. Kerth,  
Yu. G. Kolomensky, G. Kukartsev, G. Lynch, L. M. Mir, P. J. Oddone, T. J. Orimoto, M. Pripstein,  
N. A. Roe, M. T. Ronan, V. G. Shelkov, W. A. Wenzel

*Lawrence Berkeley National Laboratory and University of California, Berkeley, CA 94720, USA*

M. Barrett, K. E. Ford, T. J. Harrison, A. J. Hart, C. M. Hawkes, S. E. Morgan, A. T. Watson

*University of Birmingham, Birmingham, B15 2TT, United Kingdom*

M. Fritsch, K. Goetzen, T. Held, H. Koch, B. Lewandowski, M. Pelizaeus, M. Steinke  
*Ruhr Universität Bochum, Institut für Experimentalphysik 1, D-44780 Bochum, Germany*

J. T. Boyd, N. Chevalier, W. N. Cottingham, M. P. Kelly, T. E. Latham, F. F. Wilson

*University of Bristol, Bristol BS8 1TL, United Kingdom*

T. Cuhadar-Donszelmann, C. Hearty, N. S. Knecht, T. S. Mattison, J. A. McKenna, D. Thiessen

*University of British Columbia, Vancouver, BC, Canada V6T 1Z1*

A. Khan, P. Kyberd, L. Teodorescu

*Brunel University, Uxbridge, Middlesex UB8 3PH, United Kingdom*

A. E. Blinov, V. E. Blinov, V. P. Druzhinin, V. B. Golubev, V. N. Ivanchenko, E. A. Kravchenko,  
A. P. Onuchin, S. I. Serebnyakov, Yu. I. Skovpen, E. P. Solodov, A. N. Yushkov

*Budker Institute of Nuclear Physics, Novosibirsk 630090, Russia*

D. Best, M. Bruinsma, M. Chao, I. Eschrich, D. Kirkby, A. J. Lankford, M. Mandelkern, R. K. Mommsen,  
W. Roethel, D. P. Stoker

*University of California at Irvine, Irvine, CA 92697, USA*

C. Buchanan, B. L. Hartfiel

*University of California at Los Angeles, Los Angeles, CA 90024, USA*

S. D. Foulkes, J. W. Gary, B. C. Shen, K. Wang

*University of California at Riverside, Riverside, CA 92521, USA*

- D. del Re, H. K. Hadavand, E. J. Hill, D. B. MacFarlane, H. P. Paar, Sh. Rahatlou, V. Sharma  
*University of California at San Diego, La Jolla, CA 92093, USA*
- J. W. Berryhill, C. Campagnari, B. Dahmes, O. Long, A. Lu, M. A. Mazur, J. D. Richman, W. Verkerke  
*University of California at Santa Barbara, Santa Barbara, CA 93106, USA*
- T. W. Beck, A. M. Eisner, C. A. Heusch, J. Kroseberg, W. S. Lockman, G. Nesom, T. Schalk,  
B. A. Schumm, A. Seiden, P. Spradlin, D. C. Williams, M. G. Wilson  
*University of California at Santa Cruz, Institute for Particle Physics, Santa Cruz, CA 95064, USA*
- J. Albert, E. Chen, G. P. Dubois-Felsmann, A. Dvoretzki, D. G. Hitlin, I. Narsky, T. Piatenko,  
F. C. Porter, A. Ryd, A. Samuel, S. Yang  
*California Institute of Technology, Pasadena, CA 91125, USA*
- S. Jayatileke, G. Mancinelli, B. T. Meadows, M. D. Sokoloff  
*University of Cincinnati, Cincinnati, OH 45221, USA*
- T. Abe, F. Blanc, P. Bloom, S. Chen, W. T. Ford, U. Nauenberg, A. Olivas, P. Rankin, J. G. Smith,  
J. Zhang, L. Zhang  
*University of Colorado, Boulder, CO 80309, USA*
- A. Chen, J. L. Harton, A. Soffer, W. H. Toki, R. J. Wilson, Q. Zeng  
*Colorado State University, Fort Collins, CO 80523, USA*
- D. Altenburg, T. Brandt, J. Brose, M. Dickopp, E. Feltresi, A. Hauke, H. M. Lacker, R. Müller-Pfefferkorn,  
R. Nogowski, S. Otto, A. Petzold, J. Schubert, K. R. Schubert, R. Schwierz, B. Spaan, J. E. Sundermann  
*Technische Universität Dresden, Institut für Kern- und Teilchenphysik, D-01062 Dresden, Germany*
- D. Bernard, G. R. Bonneaud, F. Brochard, P. Grenier, S. Schrenk, Ch. Thiebaux, G. Vasileiadis, M. Verderi  
*Ecole Polytechnique, LLR, F-91128 Palaiseau, France*
- D. J. Bard, P. J. Clark, D. Lavin, F. Muheim, S. Playfer, Y. Xie  
*University of Edinburgh, Edinburgh EH9 3JZ, United Kingdom*
- M. Andreotti, V. Azzolini, D. Bettoni, C. Bozzi, R. Calabrese, G. Cibinetto, E. Luppi, M. Negrini,  
L. Piemontese, A. Sarti  
*Università di Ferrara, Dipartimento di Fisica and INFN, I-44100 Ferrara, Italy*
- E. Treadwell  
*Florida A&M University, Tallahassee, FL 32307, USA*
- F. Anulli, R. Baldini-Ferrolì, A. Calcaterra, R. de Sangro, G. Finocchiaro, P. Patteri, I. M. Peruzzi,  
M. Piccolo, A. Zallo  
*Laboratori Nazionali di Frascati dell'INFN, I-00044 Frascati, Italy*
- A. Buzzo, R. Capra, R. Contri, G. Crosetti, M. Lo Vetere, M. Macri, M. R. Monge, S. Passaggio,  
C. Patrignani, E. Robutti, A. Santroni, S. Tosi  
*Università di Genova, Dipartimento di Fisica and INFN, I-16146 Genova, Italy*
- S. Bailey, G. Brandenburg, K. S. Chaisanguanthum, M. Morii, E. Won  
*Harvard University, Cambridge, MA 02138, USA*

R. S. Dubitzky, U. Langenegger

*Universität Heidelberg, Physikalisches Institut, Philosophenweg 12, D-69120 Heidelberg, Germany*

W. Bhimji, D. A. Bowerman, P. D. Dauncey, U. Egede, J. R. Gaillard, G. W. Morton, J. A. Nash,  
M. B. Nikolich, G. P. Taylor

*Imperial College London, London, SW7 2AZ, United Kingdom*

M. J. Charles, G. J. Grenier, U. Mallik

*University of Iowa, Iowa City, IA 52242, USA*

J. Cochran, H. B. Crawley, J. Lamsa, W. T. Meyer, S. Prell, E. I. Rosenberg, A. E. Rubin, J. Yi

*Iowa State University, Ames, IA 50011-3160, USA*

M. Biasini, R. Covarelli, M. Pioppi

*Università di Perugia, Dipartimento di Fisica and INFN, I-06100 Perugia, Italy*

M. Davier, X. Giroux, G. Grosdidier, A. Höcker, S. Laplace, F. Le Diberder, V. Lepeltier, A. M. Lutz,  
T. C. Petersen, S. Plaszczynski, M. H. Schune, L. Tantot, G. Wormser

*Laboratoire de l'Accélérateur Linéaire, F-91898 Orsay, France*

C. H. Cheng, D. J. Lange, M. C. Simani, D. M. Wright

*Lawrence Livermore National Laboratory, Livermore, CA 94550, USA*

A. J. Bevan, C. A. Chavez, J. P. Coleman, I. J. Forster, J. R. Fry, E. Gabathuler, R. Gamet,  
D. E. Hutchcroft, R. J. Parry, D. J. Payne, R. J. Sloane, C. Touramanis

*University of Liverpool, Liverpool L69 7ZE, United Kingdom*

J. J. Back,<sup>1</sup> C. M. Cormack, P. F. Harrison,<sup>1</sup> F. Di Lodovico, G. B. Mohanty<sup>1</sup>

*Queen Mary, University of London, E1 4NS, United Kingdom*

C. L. Brown, G. Cowan, R. L. Flack, H. U. Flaecher, M. G. Green, P. S. Jackson, T. R. McMahon,  
S. Ricciardi, F. Salvatore, M. A. Winter

*University of London, Royal Holloway and Bedford New College, Egham, Surrey TW20 0EX,  
United Kingdom*

D. Brown, C. L. Davis

*University of Louisville, Louisville, KY 40292, USA*

J. Allison, N. R. Barlow, R. J. Barlow, P. A. Hart, M. C. Hodgkinson, G. D. Lafferty, A. J. Lyon,  
J. C. Williams

*University of Manchester, Manchester M13 9PL, United Kingdom*

A. Farbin, W. D. Hulsbergen, A. Jawahery, D. Kovalskyi, C. K. Lae, V. Lillard, D. A. Roberts

*University of Maryland, College Park, MD 20742, USA*

G. Blaylock, C. Dallapiccola, K. T. Flood, S. S. Hertzbach, R. Kofler, V. B. Koptchev, T. B. Moore,  
S. Saremi, H. Staengle, S. Willocq

*University of Massachusetts, Amherst, MA 01003, USA*

---

<sup>1</sup>Now at Department of Physics, University of Warwick, Coventry, United Kingdom

R. Cowan, G. Sciolla, S. J. Sekula, F. Taylor, R. K. Yamamoto  
*Massachusetts Institute of Technology, Laboratory for Nuclear Science, Cambridge, MA 02139, USA*

D. J. J. Mangeol, P. M. Patel, S. H. Robertson  
*McGill University, Montréal, QC, Canada H3A 2T8*

A. Lazzaro, V. Lombardo, F. Palombo  
*Università di Milano, Dipartimento di Fisica and INFN, I-20133 Milano, Italy*

J. M. Bauer, L. Cremaldi, V. Eschenburg, R. Godang, R. Kroeger, J. Reidy, D. A. Sanders, D. J. Summers,  
H. W. Zhao  
*University of Mississippi, University, MS 38677, USA*

S. Brunet, D. Côté, P. Taras  
*Université de Montréal, Laboratoire René J. A. Lévesque, Montréal, QC, Canada H3C 3J7*

H. Nicholson  
*Mount Holyoke College, South Hadley, MA 01075, USA*

N. Cavallo,<sup>2</sup> F. Fabozzi,<sup>2</sup> C. Gatto, L. Lista, D. Monorchio, P. Paolucci, D. Piccolo, C. Sciacca  
*Università di Napoli Federico II, Dipartimento di Scienze Fisiche and INFN, I-80126, Napoli, Italy*

M. Baak, H. Bulten, G. Raven, H. L. Snoek, L. Wilden  
*NIKHEF, National Institute for Nuclear Physics and High Energy Physics, NL-1009 DB Amsterdam,  
The Netherlands*

C. P. Jessop, J. M. LoSecco  
*University of Notre Dame, Notre Dame, IN 46556, USA*

T. Allmendinger, K. K. Gan, K. Honscheid, D. Hufnagel, H. Kagan, R. Kass, T. Pulliam, A. M. Rahimi,  
R. Ter-Antonyan, Q. K. Wong  
*Ohio State University, Columbus, OH 43210, USA*

J. Brau, R. Frey, O. Igonkina, C. T. Potter, N. B. Sinev, D. Strom, E. Torrence  
*University of Oregon, Eugene, OR 97403, USA*

F. Colecchia, A. Dorigo, F. Galeazzi, M. Margoni, M. Morandin, M. Posocco, M. Rotondo, F. Simonetto,  
R. Stroili, G. Tiozzo, C. Voci  
*Università di Padova, Dipartimento di Fisica and INFN, I-35131 Padova, Italy*

M. Benayoun, H. Briand, J. Chauveau, P. David, Ch. de la Vaissière, L. Del Buono, O. Hamon,  
M. J. J. John, Ph. Leruste, J. Malcles, J. Ocariz, M. Pivk, L. Roos, S. T'Jampens, G. Therin  
*Universités Paris VI et VII, Laboratoire de Physique Nucléaire et de Hautes Energies, F-75252 Paris,  
France*

P. F. Manfredi, V. Re  
*Università di Pavia, Dipartimento di Elettronica and INFN, I-27100 Pavia, Italy*

---

<sup>2</sup>Also with Università della Basilicata, Potenza, Italy

P. K. Behera, L. Gladney, Q. H. Guo, J. Panetta  
*University of Pennsylvania, Philadelphia, PA 19104, USA*

C. Angelini, G. Batignani, S. Bettarini, M. Bondioli, F. Bucci, G. Calderini, M. Carpinelli, F. Forti,  
M. A. Giorgi, A. Lusiani, G. Marchiori, F. Martinez-Vidal,<sup>3</sup> M. Morganti, N. Neri, E. Paoloni, M. Rama,  
G. Rizzo, F. Sandrelli, J. Walsh  
*Università di Pisa, Dipartimento di Fisica, Scuola Normale Superiore and INFN, I-56127 Pisa, Italy*

M. Haire, D. Judd, K. Paick, D. E. Wagoner  
*Prairie View A&M University, Prairie View, TX 77446, USA*

N. Danielson, P. Elmer, Y. P. Lau, C. Lu, V. Miftakov, J. Olsen, A. J. S. Smith, A. V. Telnov  
*Princeton University, Princeton, NJ 08544, USA*

F. Bellini, G. Cavoto,<sup>4</sup> R. Faccini, F. Ferrarotto, F. Ferroni, M. Gaspero, L. Li Gioi, M. A. Mazzoni,  
S. Morganti, M. Pierini, G. Piredda, F. Safai Tehrani, C. Voena  
*Università di Roma La Sapienza, Dipartimento di Fisica and INFN, I-00185 Roma, Italy*

S. Christ, G. Wagner, R. Waldi  
*Universität Rostock, D-18051 Rostock, Germany*

T. Adye, N. De Groot, B. Franek, N. I. Geddes, G. P. Gopal, E. O. Olaiya  
*Rutherford Appleton Laboratory, Chilton, Didcot, Oxon, OX11 0QX, United Kingdom*

R. Aleksan, S. Emery, A. Gaidot, S. F. Ganzhur, P.-F. Giraud, G. Hamel de Monchenault, W. Kozanecki,  
M. Legendre, G. W. London, B. Mayer, G. Schott, G. Vasseur, Ch. Yèche, M. Zito  
*DSM/Daphnia, CEA/Saclay, F-91191 Gif-sur-Yvette, France*

M. V. Purohit, A. W. Weidemann, J. R. Wilson, F. X. Yumiceva  
*University of South Carolina, Columbia, SC 29208, USA*

D. Aston, R. Bartoldus, N. Berger, A. M. Boyarski, O. L. Buchmueller, R. Claus, M. R. Convery,  
M. Cristinziani, G. De Nardo, D. Dong, J. Dorfan, D. Dujmic, W. Dunwoodie, E. E. Elsen, S. Fan,  
R. C. Field, T. Glanzman, S. J. Gowdy, T. Hadig, V. Halyo, C. Hast, T. Hryn'ova, W. R. Innes,  
M. H. Kelsey, P. Kim, M. L. Kocian, D. W. G. S. Leith, J. Libby, S. Luitz, V. Luth, H. L. Lynch,  
H. Marsiske, R. Messner, D. R. Muller, C. P. O'Grady, V. E. Ozcan, A. Perazzo, M. Perl, S. Petrak,  
B. N. Ratcliff, A. Roodman, A. A. Salnikov, R. H. Schindler, J. Schwiening, G. Simi, A. Snyder, A. Soha,  
J. Stelzer, D. Su, M. K. Sullivan, J. Va'vra, S. R. Wagner, M. Weaver, A. J. R. Weinstein,  
W. J. Wisniewski, M. Wittgen, D. H. Wright, A. K. Yarritu, C. C. Young  
*Stanford Linear Accelerator Center, Stanford, CA 94309, USA*

P. R. Burchat, A. J. Edwards, T. I. Meyer, B. A. Petersen, C. Roat  
*Stanford University, Stanford, CA 94305-4060, USA*

S. Ahmed, M. S. Alam, J. A. Ernst, M. A. Saeed, M. Saleem, F. R. Wappler  
*State University of New York, Albany, NY 12222, USA*

---

<sup>3</sup>Also with IFIC, Instituto de Física Corpuscular, CSIC-Universidad de Valencia, Valencia, Spain

<sup>4</sup>Also with Princeton University, Princeton, USA

W. Bugg, M. Krishnamurthy, S. M. Spanier  
*University of Tennessee, Knoxville, TN 37996, USA*

R. Eckmann, H. Kim, J. L. Ritchie, A. Satpathy, R. F. Schwitters  
*University of Texas at Austin, Austin, TX 78712, USA*

J. M. Izen, I. Kitayama, X. C. Lou, S. Ye  
*University of Texas at Dallas, Richardson, TX 75083, USA*

F. Bianchi, M. Bona, F. Gallo, D. Gamba  
*Università di Torino, Dipartimento di Fisica Sperimentale and INFN, I-10125 Torino, Italy*

L. Bosisio, C. Cartaro, F. Cossutti, G. Della Ricca, S. Dittongo, S. Grancagnolo, L. Lanceri, P. Poropat,<sup>5</sup>  
L. Vitale, G. Vuagnin  
*Università di Trieste, Dipartimento di Fisica and INFN, I-34127 Trieste, Italy*

R. S. Panvini  
*Vanderbilt University, Nashville, TN 37235, USA*

Sw. Banerjee, C. M. Brown, D. Fortin, P. D. Jackson, R. Kowalewski, J. M. Roney, R. J. Sobie  
*University of Victoria, Victoria, BC, Canada V8W 3P6*

H. R. Band, B. Cheng, S. Dasu, M. Datta, A. M. Eichenbaum, M. Graham, J. J. Hollar, J. R. Johnson,  
P. E. Kutter, H. Li, R. Liu, A. Mihalyi, A. K. Mohapatra, Y. Pan, R. Prepost, P. Tan, J. H. von  
Wimmersperg-Toeller, J. Wu, S. L. Wu, Z. Yu  
*University of Wisconsin, Madison, WI 53706, USA*

M. G. Greene, H. Neal  
*Yale University, New Haven, CT 06511, USA*

---

<sup>5</sup>Deceased

# 1 Introduction

Recently several experimental groups have reported observations of a new, manifestly exotic ( $B=1$ ,  $S=1$ ) baryon resonance, called the  $\Theta^+(1540)$  [1]-[7], with an unusually narrow width ( $\Gamma < 8 \text{ MeV}/c^2$ ) for a particle in this mass range that has open channels to strong decay. Also, the NA49 experiment reported evidence for an additional narrow exotic ( $B=1$ ,  $Q=S=-2$ ) state, called  $\Xi^{--}$ , as well as corresponding  $\Xi^0$  state, with masses close to  $1862 \text{ MeV}/c^2$  [8]. More recently the H1 collaboration reported a narrow ( $\Gamma < 30 \text{ MeV}/c^2$ ) exotic charmed ( $B=1$ ,  $C=-1$ ) resonance,  $\Theta_c^0$ , with a mass of  $3099 \text{ MeV}/c^2$ . The simplest quark assignments consistent with the quantum numbers of  $\Theta^+$ ,  $\Xi^{--}$  and  $\Theta_c^0$  are  $(udud\bar{s})$ ,  $(dsds\bar{u})$  and  $(udud\bar{c})$ , respectively; therefore these observed states are regarded as pentaquark candidates.

These results have prompted a surge of pentaquark searches in experimental data of many kinds, mostly with negative results [10]. Several theoretical models [11, 12, 13] have been proposed to describe possible pentaquark structure. They predict that the lowest mass states containing  $u$ ,  $d$  and  $s$  quarks should occupy a spin-1/2 antidecuplet and octet, as illustrated in Fig. 1. Predictions for the masses of the unobserved  $N$  and  $\Sigma$  states vary;  $M_N$  might be anywhere between  $\sim 150 \text{ MeV}/c^2$  below  $M_\Theta$  and  $\sim M_\Xi$ , and  $M_\Sigma$  anywhere between  $\sim M_\Theta$  and  $\sim 150 \text{ MeV}/c^2$  above  $M_\Xi$ . In order to distinguish pentaquarks from ordinary baryons, we adopt a notation that has names corresponding to ordinary baryons with similar  $s$  quark content, plus a subscript 5. For example, the  $\Xi_5^-$  pentaquark ( $dss(u\bar{u} + d\bar{d})$ ) corresponds to the ordinary  $\Xi^-$  ( $dss$ ) baryon.

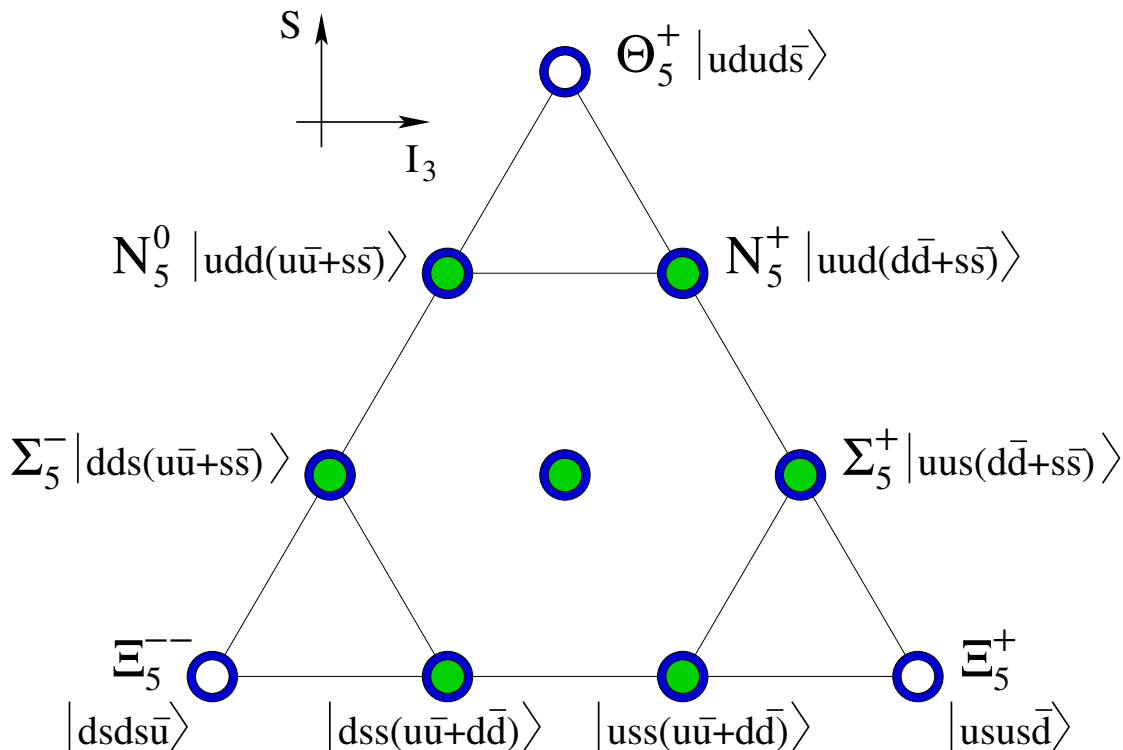


Figure 1: Quark structure of the antidecuplet (annuli) and octet (filled circles) that are generally assumed for the lowest-mass pentaquarks. Strangeness increases in the vertical direction and the third component of isospin in the horizontal.

Although experiments with a baryon in the beam or the target might have some advantage in pentaquark production,  $e^+e^-$  interactions are also known for democratic production of hadrons. Baryons with nonzero beauty, charm, strangeness (up to three units) and/or orbital angular momentum have been observed with production rates that appear to depend on the mass and spin, but not quark content. If pentaquarks are produced similarly, then one might expect a pentaquark rate as high as that for an ordinary baryon of the same mass and spin, i.e. about  $8 \times 10^{-4} \Theta_5^+$  and about  $4 \times 10^{-5} \Xi_5^{--}$  per  $e^+e^- \rightarrow$  hadrons event at  $\sqrt{s} = 10.58$  GeV [15]. Decays of  $B$  mesons are also known to produce a rather high rate of baryons and so provide another fertile hunting ground. In both cases we expect any set of pentaquark states forming a multiplet of approximately equal mass to be produced at roughly equal rates, so that access to all narrow states is available.

Here we describe a program of inclusive searches for the reported states and also the other members of the hypothetical antidecuplet and octet in data from the *BABAR* experiment, which include both  $e^+e^- \rightarrow q\bar{q}$ ,  $q = udsc$ , events and the production of  $\Upsilon(4S)$  mesons, which decay into  $B\bar{B}$  pairs. We have concentrated on decay modes involving strange particles and protons, which are easily reconstructed in our detector. All states except the  $N_5$  have nonzero strangeness, and the  $N_5$  and  $\Sigma_5$  have hidden strangeness divided in some way between the octet and antidecuplet states. Since the production mechanism, and hence the momentum spectra, for pentaquarks is unknown, we consider differential production cross sections  $d\sigma/dp^*$  per unit momentum  $p^*$  in the  $e^+e^-$  center-of-mass (c.m.) frame, which are to first order independent of any model, and applicable to the sum of all production processes at  $\sqrt{s} = 10.58$  GeV. After describing some common aspects of the analyses in section 2, we describe searches in three classes of decay modes in the next three sections. Upper limits on pentaquark production are discussed in section 6, and we summarize the results in section 7.

## 2 Data and Simulation

The data sample used in the analysis comprises the runs of the *BABAR* experiment through 2003, and amounts to an integrated luminosity of  $123 \text{ fb}^{-1}$ , roughly 90% (10%) of which was recorded on (below) the  $\Upsilon(4S)$  resonance at a c.m. energy of  $\sqrt{s} = 10.58$  (10.54) GeV. The *BABAR* detector is described in detail in Ref. [14]. Here we use charged tracks reconstructed in the 5-layer silicon vertex detector (SVT) and the 40-layer drift chamber (DCH), and identified using a combination of energy loss measured in these two subdetectors and Cherenkov angles measured in the detector of internally reflected Cherenkov radiation (DIRC). The charged particle momentum resolution is given by  $(\delta p_T/p_T)^2 = (0.0013p_T)^2 + 0.0045^2$ , where  $p_T$  is the momentum transverse to the beam axis in GeV/ $c$ . Loose particle identification is required on most particles, giving in each case nearly 100% efficiency with a sizable background reduction. Tighter requirements are made where noted, giving identification efficiencies ranging from 80–99% and background rejection factors of 12–100. Photons are detected by a CsI(Tl) electromagnetic calorimeter (EMC) with an energy resolution of  $\sigma(E)/E = 0.023 \cdot (E/\text{GeV})^{-1/4} \oplus 0.019$ . Our invariant mass resolution for a given decay mode is better than that of any experiment reporting the observation of a pentaquark candidate with that mode available.

Minimal hadronic event selection is performed, as we wish to be as inclusive as possible and maintain maximum signal efficiency. We simply require three reconstructed charged tracks in the event. The vast majority of the events are hadronic; lepton-pair events are expected to contribute negligible background in the signal regions; two-photon events and events with a hard initial-state photon contribute only at low momenta. The acceptance for a pentaquark signal from any of these

sources is well understood; if a signal is found, we can attempt to isolate the source with cuts on the event properties.

Samples of simulated  $e^+e^- \rightarrow q\bar{q}$ , where  $q = udsc$ , are generated using the JETSET [16] Monte Carlo generator combined with a detailed simulation of the *BABAR* detector, in order to study backgrounds and “control” particles – known resonances with similar masses and decay modes to the pentaquark in question. By comparing with the same particles reconstructed in the data, we verify the simulation of the invariant mass resolutions and biases of the detector, an essential ingredient in the evaluation of any new signal, or limit where no signal is seen.

In order to evaluate pentaquark reconstruction efficiencies, we simulate pentaquark signals within our standard software with special parameter settings of the JETSET generator. For each pentaquark state we take an existing baryon as a stand-in, change its mass and width to match the desired pentaquark properties, and force a particular decay mode, with all other JETSET parameters left unchanged. The generator thus gives the stand-in particles a momentum spectrum based on the pentaquark mass, but the stand-in flavor. We make no attempt here to conserve flavor in the production process, as we are only concerned with providing an appropriate number and distribution of additional particles in the event. We do not know the production mechanism for such five-quark states; however, to make the measurement we only need the efficiency as a function of the relevant variables, in this case momentum and polar angle in the laboratory frame, so any smooth distribution that covers the entire range of these variables is sufficient. Effects such as the type, multiplicity and proximity of other particles in the event can be studied by using different stand-in baryons; such effects are found to be smaller than the other systematic uncertainties. The stand-in particles used to generate our signal samples are summarized in Table 1.

Table 1: Baryons used in the simulation to generate pentaquark signal samples.

Pentaquark Signal mode	Existing Baryon Used	Mass (MeV/ $c^2$ )	Width (MeV/ $c^2$ )	# of Events
$\Theta_5^+ \rightarrow pK_S^0$	$\Delta^+$	1540	1	120,000
$\Xi_5^{--} \rightarrow \Xi^- \pi^-$	$\Delta^{++}$	1862	1	120,000
	$\Sigma_c^{++}$	1862	1	98,000
$\Xi_5^0 \rightarrow \Xi^- \pi^+$	$\Xi^{*0}$	1862	1	60,000
$\Sigma_5^0 \rightarrow \Xi^- K^+$	$\Xi^{*0}$	1862	1	120,000
$\Xi_5^- \rightarrow \Lambda^0 K^-$	$\Xi^{*-}$	1862	1	29,000
$\Xi_5^+ / N_5^+ \rightarrow \Lambda^0 K^+$	$\Xi^{*+}$	1862	1	29,000
$\Xi_5^0 \rightarrow \Lambda^0 K_S^0$	$\Xi^{*0}$	1862	1	29,000
$\Xi_5^- \rightarrow \Sigma^0 K^-$	$\Xi^{*-}$	1862	1	27,000
$\Xi_5^+ / N_5^+ \rightarrow \Sigma^0 K^+$	$\Xi^{*+}$	1862	1	27,000
$\Xi_5^0 \rightarrow \Sigma^0 K_S^0$	$\Xi^{*0}$	1862	1	25,000

### 3 Search for the $\Theta_5^+(1540) \rightarrow pK_s^0$

We reconstruct  $\Theta_5^+$  candidates in the  $pK_s^0$  decay mode, where  $K_s^0 \rightarrow \pi^-\pi^+$ , with selection criteria designed for high efficiency and low bias against any production mechanism. A sample of  $K_s^0$  candidates is obtained from all pairs of oppositely charged tracks passing loose pion identification requirements that pass within 6 mm of each other. Each pair is required to: have a total momentum vector extrapolating within 6 mm (32 mm) of the interaction point (IP) in the plane transverse to (along) the beam direction; have a positive flight distance, defined as the projection on the candidate momentum direction of a vector from its point of closest approach to the beam axis to its decay point; and have an invariant mass within 10 MeV/ $c^2$  of the nominal  $K_s^0$  mass. We also require the helicity angle  $\theta_H$  of the candidate, defined as the angle between the  $\pi^+$  and the reconstructed  $\pi^+\pi^-$  flight direction in the  $\pi^+\pi^-$  rest frame, to satisfy  $|\cos\theta_H| < 0.8$ , eliminating background from  $\Lambda^0$  decays and photon conversions and reducing combinatoric background.

We combine the surviving  $K_s^0$  candidates with identified  $p$  and  $\bar{p}$  tracks that extrapolate within 15 mm (10 cm) of the IP in the plane transverse to (along) the beam direction. The simulated signal reconstruction efficiency varies with  $p^*$ , the  $pK_s^0$  momentum in the  $e^+e^-$  c.m. frame, from 13% at low  $p^*$  to 22% at high  $p^*$ . The invariant mass distribution of these pairs is shown in Fig. 2. There is a clear peak at 2285 MeV/ $c^2$  from  $\Lambda_c^+ \rightarrow pK_s^0$  but no other sharp structure. The  $\Lambda_c^+$  peak (upper right plot) shows a mass resolution of better than 6 MeV/ $c^2$  and contains roughly 52,000 entries, demonstrating our sensitivity to the presence of a narrow resonance. The lower plots zoom in on the mass ranges 1400–1600 and 1600–1800 MeV/ $c^2$ . The  $\Theta_5^+$  has been reported at values between 1520 and 1540 MeV/ $c^2$ . There is no enhancement in our data anywhere in this region. The  $pK_s^0$  decay mode is also possible for the  $\Sigma_5^+$  states, whose masses might be expected to be between that of the  $\Theta_5^+$  and about 2000 MeV/ $c^2$  depending on their strange quark content. There is no sign of a narrow resonance anywhere in this region.

We consider several additional criteria that might enhance a pentaquark signal. More stringent requirements on the flight distance of the  $K_s^0$  candidate give a much cleaner  $K_s^0$  sample at the expense of efficiency at low momentum. This enhances the  $\Lambda_c^+$  signal to noise, but does not reveal any additional structure. If a pentaquark is produced in an  $e^+e^-$  annihilation event, then there must also be an antibaryon (or anti-pentaquark) in the event, among whose decay products is either an antiproton or antineutron. In the case of the  $\Theta_5^+$  decaying to  $pK_s^0$ , the  $K_s^0$  must have been a  $K^0$  rather than a  $\bar{K}^0$ , and there must be a compensating particle in the event with strangeness  $-1$ , which might often be a  $K^-$ . We consider all subsets of the  $pK_s^0$  combinations for which there is also at least one loosely identified  $K^-$  and/or  $\bar{p}$  track in the event. In all cases the data quantity is reduced, the  $\Lambda_c^+$  signal is still visible and there is no sign of a pentaquark peak. Following work by the CLAS and NA49 experiments [3, 8], we reconstruct a possible  $N^*(2400) \rightarrow K^-K_s^0p$  using the selected  $pK_s^0$  pairs and an additional loosely identified  $K^-$  candidate. We observe no  $N^*$  peak in our data. Considering various  $K^-K_s^0p$  mass ranges, the  $pK_s^0$  mass distribution for  $K^-K_s^0p$  masses near 2400 MeV/ $c^2$  shows no pentaquark signal, and is indistinguishable from the  $pK_s^0$  mass distributions in nearby  $K^-K_s^0p$  mass ranges. Requiring in addition a recoil antiproton yields similar results.

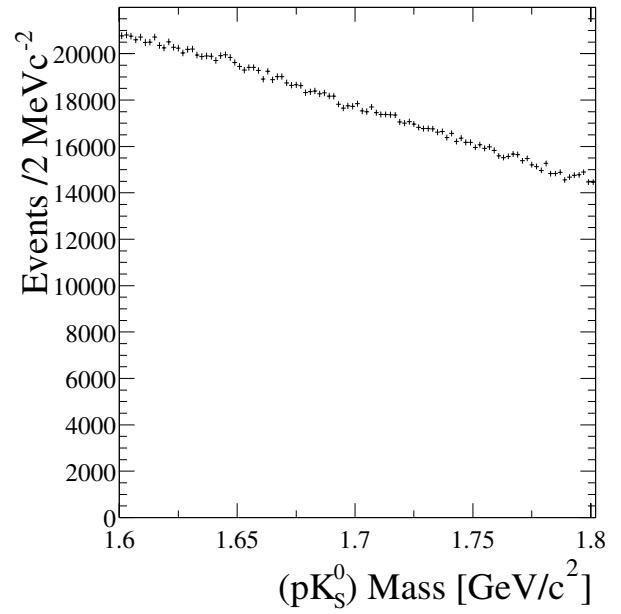
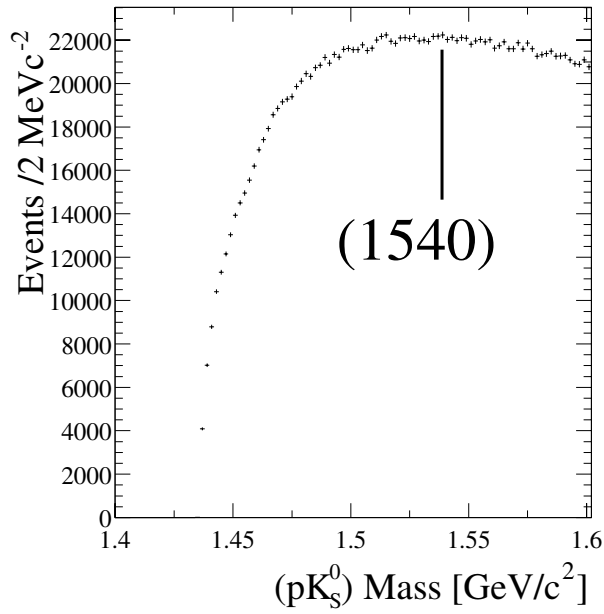
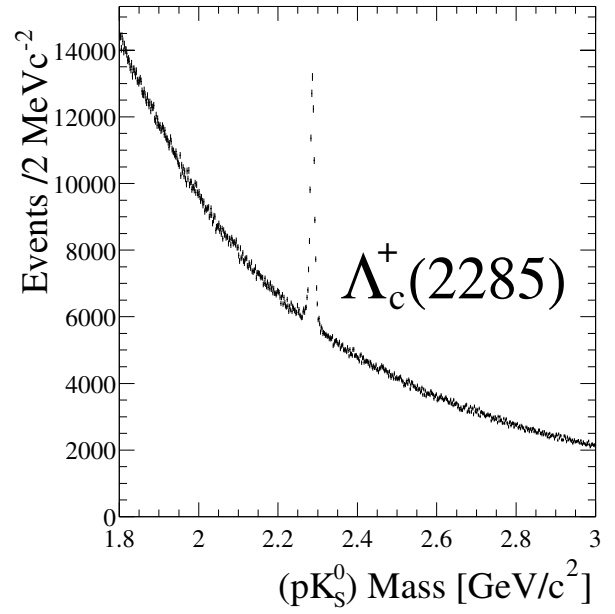
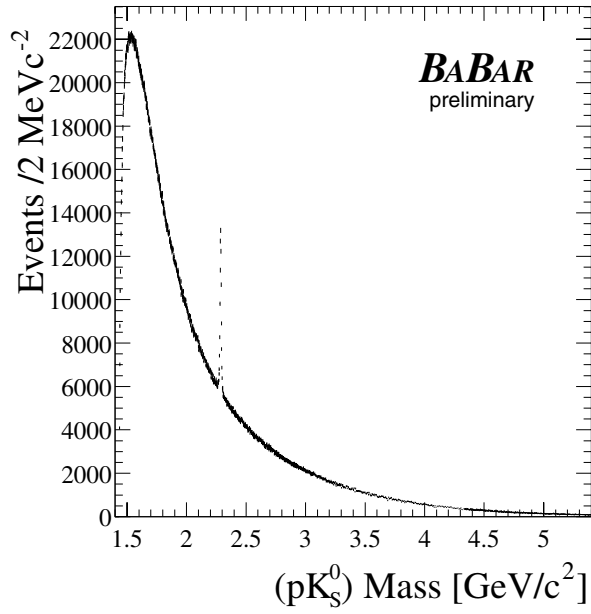


Figure 2: Distribution of the  $pK_s^0$  invariant mass for combinations satisfying all the criteria described in the text. The same data are plotted four times in different  $pK_s^0$  mass regions.

In each of the above cases we split the data into ten bins of  $p^*$ , in order to enhance our sensitivity to any production mechanism that gives a momentum spectrum different from that of our background. The bins are 500 MeV/ $c^2$  wide and cover the  $p^*$  range from zero to 5 GeV/ $c^2$ , the kinematic limit for a particle of mass 1700 MeV/ $c^2$ . The background is much smaller at higher  $p^*$ , so we are more sensitive to mechanisms that produce harder spectra. In no case is there any sign of a pentaquark signal.

We quantify these null results for the  $\Theta_5^+$ , assuming a mass of 1540 MeV/ $c^2$ . In order to reduce model dependence, we consider the ten  $p^*$  bins noted above and fit a signal plus background function to the  $pK_s^0$  invariant mass distribution in each bin. The natural width of the  $\Theta_5^+$  has not been measured; the best upper limit,  $\Gamma < 8$  MeV/ $c^2$ , is larger than our detector resolution, so we must consider the range of widths up to this value. We use a P-wave Breit-Wigner lineshape multiplied by a phase-space factor and convolved with a resolution function derived from the  $\Lambda_c^+$  data and simulation. The latter is a sum of two Gaussian distributions with a common center and an overall rms ranging from 2.5 MeV/ $c^2$  at low  $p^*$  to 1.8 MeV/ $c^2$  at high  $p^*$ ; this is narrower than for the  $\Lambda_c^+$  due to the proximity of the  $\Theta_5^+$  (1540) to threshold. For the natural width we consider two possibilities, 1 MeV/ $c^2$  and 8 MeV/ $c^2$ , corresponding to a very narrow state and the upper limit, respectively. The fits are performed over a wide range, from threshold to 1800 MeV/ $c^2$ , and the background function is a seventh-order polynomial times a threshold factor.

For the case of our nominal selection criteria (Fig. 2), we obtain the signal yields shown in Fig. 3. In all  $p^*$  bins the fit quality is good and the signal is consistent with zero. There is no positive trend in the data, and the roughly symmetric scatter of the points about zero indicates low momentum-dependent bias in the background function. We consider systematic effects in the fitting procedure by varying the signal and background functions and fit range; changes in the fitted signal are negligible compared with the statistical uncertainties. Other selection criteria yield similar results. Since the nominal selection gives the smallest absolute uncertainties after efficiency corrections, we use it to set upper limits on the production cross section in section 6. Varying the mass assumed for the  $\Theta_5^+$  has effects consistent with statistics; in no case do we observe a signal, and the uncertainties shown in Fig. 3 are typical.

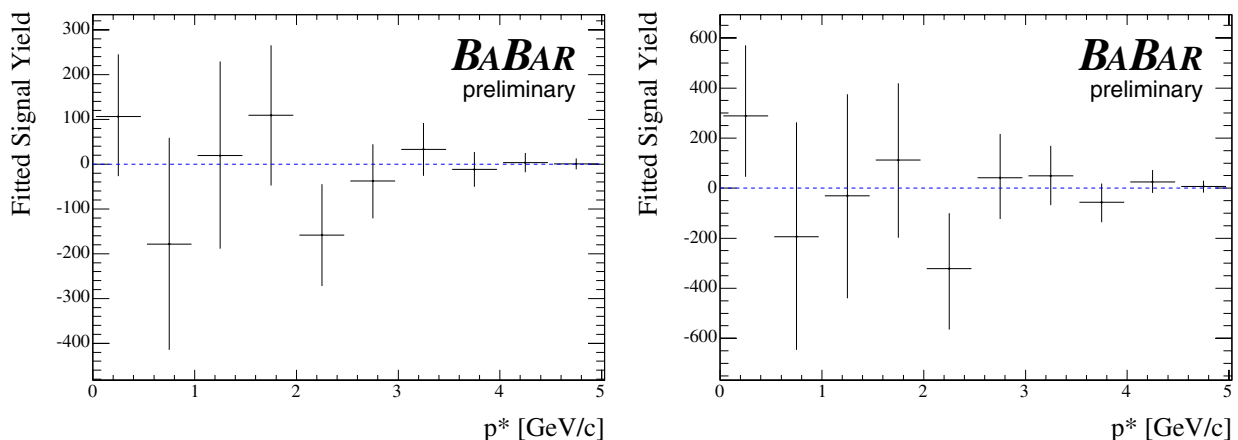


Figure 3: The  $\Theta_5^+$  signal yields extracted from the fits to the  $pK_s^0$  invariant mass distributions, assuming a  $\Theta_5^+$  mass of 1540 MeV/ $c^2$  and width  $\Gamma = 1$  MeV/ $c^2$  (left) and  $\Gamma = 8$  MeV/ $c^2$  (right).

## 4 Search for $\Xi_5^{--} \rightarrow \Xi^- \pi^-$ and $\Xi_5^0 \rightarrow \Xi^- \pi^+$

We next search for pentaquark states decaying into a  $\Xi^-$  and a charged pion, where  $\Xi^- \rightarrow \Lambda^0 \pi^-$  and  $\Lambda^0 \rightarrow p \pi^-$ , including the reported  $\Xi_5^{--}(1862)$  and  $\Xi_5^0(1862)$ . We first reconstruct  $\Lambda^0 \rightarrow p \pi^-$  candidates from all pairs of charged tracks satisfying loose proton and pion requirements. Efficient and unbiased selection criteria are again applied: the tracks must pass within 6 mm of each other; the candidate have a positive flight distance from the IP; and it must have an invariant mass within 10  $\text{MeV}/c^2$  of the nominal  $\Lambda^0$  mass. These candidates are combined with an additional negatively charged track passing loose pion identification requirements to form  $\Xi^-$  candidates. These candidates are required to form a good vertex, to have a positive flight distance from the IP, and to have an invariant mass within 20  $\text{MeV}/c^2$  of the nominal  $\Xi^-$  mass. Furthermore the flight distance of the  $\Lambda^0$  candidate from the  $\Lambda^0 \pi^-$  vertex must be positive. Finally, we combine the  $\Xi^-$  candidates with an additional charged track consistent with coming from the IP and passing loose pion identification requirements. The cosine of the angle between the reconstructed  $\Xi^-$  trajectory, extrapolated back to the IP, and the additional track is required to be less than 0.998. This last cut is especially important, since the  $\Xi^-$  is charged and has a long lifetime; if it has a long flight distance, it can produce a reconstructed track that, if combined with itself, forms a false peak in the invariant mass distribution. The simulated signal reconstruction efficiency varies from 6.5% at low  $p^*$  to 12% at high  $p^*$ .

The invariant mass distributions for  $\Xi^- \pi^-$  and  $\Xi^- \pi^+$  are shown in Figs. 4 and 5, respectively. In Fig. 5 there are clear peaks as expected for the  $\Xi^{*0}(1530)$  and  $\Xi_c^0(2470)$  baryons, but no other structure is visible. In Fig. 4 there is no visible sharp structure at all.

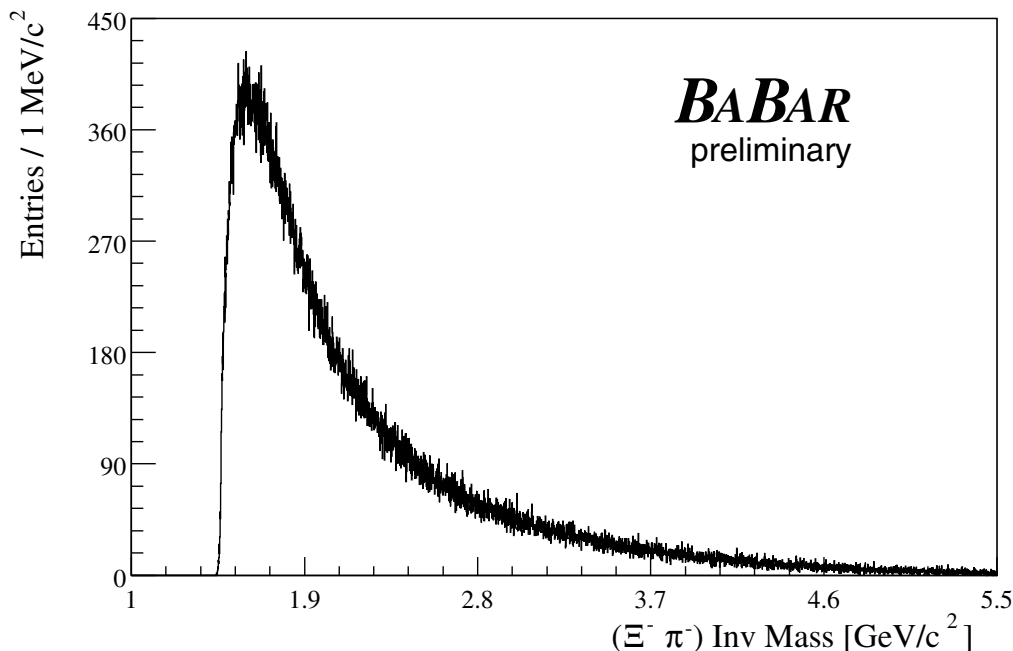


Figure 4:  $\Xi^- \pi^-$  invariant mass distribution.

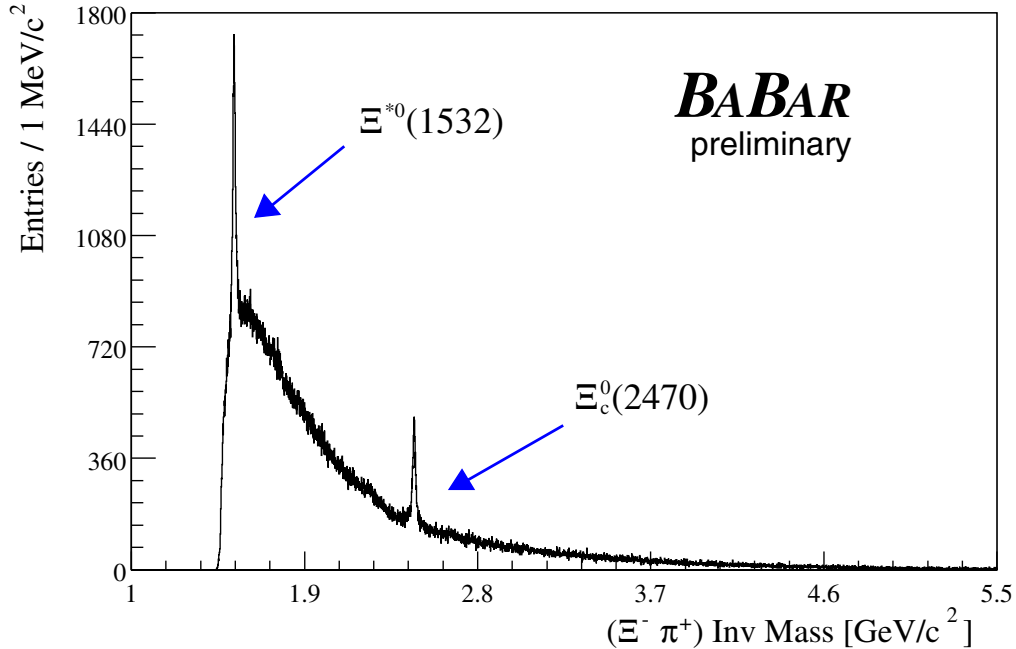


Figure 5:  $\Xi^- \pi^+$  invariant mass distribution.

As in the preceding section, we divide the  $\Xi_5^{--}$  candidates into ten bins of  $p^*$  and find no sign of a pentaquark signal in any bin. We fit a similar signal plus background function to the  $\Xi^- \pi^-$  invariant mass distribution in each bin. The resolution function is derived in this case from the  $\Xi^{*0}(1530)$  and  $\Xi_c^0(2470)$  data and simulation, and is described by a Gaussian with an rms of 8  $\text{MeV}/c^2$ . For the Breit-Wigner width we consider two possibilities, 1 and 18  $\text{MeV}/c^2$ , corresponding to a very narrow state and the upper limit on the  $\Xi_5^{--}$  width, respectively. The fits are performed over the mass range from 1760 to 1960  $\text{MeV}/c^2$ , and the background function is a seventh-order polynomial.

Fixing the  $\Xi_5^{--}$  mass to 1862  $\text{MeV}/c^2$ , we obtain the signal yields shown in Fig. 6. In all  $p^*$  bins the fit quality is good across the full mass range and the signal is consistent with zero. Systematic uncertainties on the fitting procedure are again found to be negligible compared with the statistical uncertainties, and variations of the  $\Xi_5^{--}$  mass and selection criteria give consistent results.

## 5 Search for $\Xi_5^-$ , $\Xi_5^0$ , $N_5^0$ and $N_5^+$ in the $\Lambda^0 K$ and $\Sigma^0 K$ modes

We search for pentaquark states decaying into a  $\Lambda^0 K$  or  $\Sigma^0 K$  final state, where  $K$  is a charged or neutral kaon,  $\Sigma^0 \rightarrow \Lambda^0 \gamma$  and  $\Lambda^0 \rightarrow p \pi^-$ . These final states give us access to the  $\Xi_5^-$ ,  $\Xi_5^0$ ,  $N_5^0$  and  $N_5^+$  states (see Fig. 1). The  $\Xi_5^0$  has been reported with a mass of 1862  $\text{MeV}/c^2$ , and we expect a quite similar mass for the  $\Xi_5^-$ ; since our decay modes include two strange particles, we are sensitive only to  $N_5^0$  and  $N_5^+$  states with substantial  $s\bar{s}$  content, and these might be expected somewhere between 1500 and 1900  $\text{MeV}/c^2$ .

We first reconstruct  $\Lambda^0 \rightarrow p \pi^-$  candidates from all pairs of charged tracks in which one

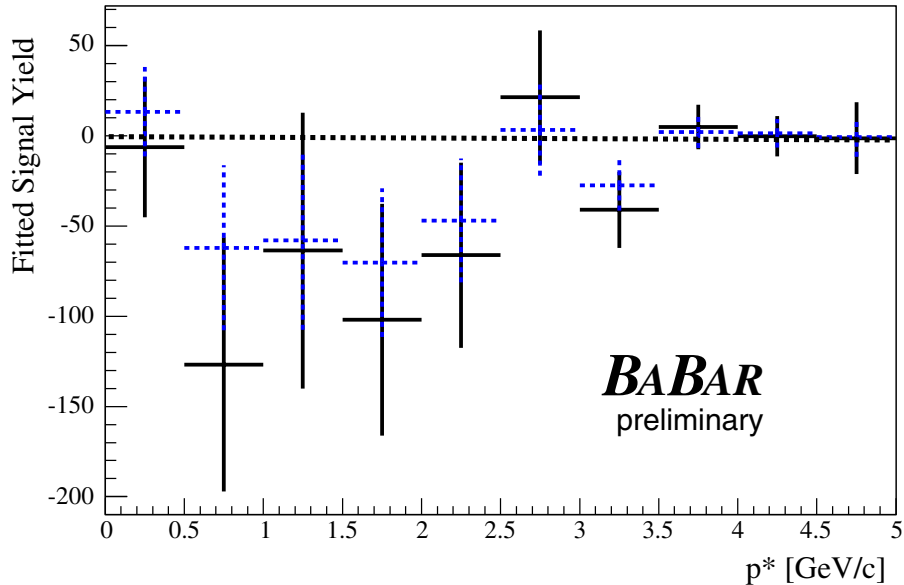


Figure 6: The  $\Xi_5^{--}$  signal yields extracted from the fits to the  $\Xi^-\pi^-$  invariant mass distributions, assuming a  $\Xi_5^{--}$  mass of 1862 MeV/ $c^2$  and width  $\Gamma = 1$  (dashed) and  $\Gamma = 18$  MeV/ $c^2$  (solid).

satisfies tight proton identification requirements, and the other loose pion identification. The pairs are required to form a good vertex, to have an angle between their flight direction (line from the IP to the vertex) and total momentum at the vertex less than 200 mrad, and to have an invariant mass within 20 MeV/ $c^2$  of the nominal  $\Lambda^0$  mass. To reconstruct  $\Sigma^0$  candidates, The  $\Lambda^0$  candidates are combined with neutral (not associated with any charged track) calorimetric energy deposits of at least 80 MeV that do not pair with any other neutral deposit to form a  $\pi^0$  candidate. We require a mass difference  $M_{p\pi\gamma} - M_{p\pi}$  within 20 MeV/ $c^2$  of the nominal  $M_{\Sigma^0} - M_{\Lambda^0}$  value. Similarly,  $K_S^0$  candidates are reconstructed from pairs of oppositely charged tracks forming a good vertex, having an angle between their flight direction and total momentum less than 30 mrad, and having an invariant mass within 4.5 MeV/ $c^2$  of the nominal  $K_S^0$  mass. Charged kaon candidates are required to be consistent with coming from the IP and to pass tight kaon identification requirements. The simulated signal reconstruction efficiencies vary from 0.5% for the  $\Sigma^0 K_S^0$  mode to 10% for the  $\Lambda^0 K^\pm$  modes at low  $p^*$ , and increase to 3% and 25%, respectively, at high  $p^*$ .

We find a substantial  $p^*$  dependence in the structure of the invariant mass distributions, and so we show them in four  $p^*$  bins, for  $\Lambda^0 K^+$ ,  $\Lambda^0 K^-$  and  $\Lambda^0 K_S^0$  combinations in Figs. 7, 8 and 9, respectively, and for  $\Sigma^0 K^+$ ,  $\Sigma^0 K^-$  and  $\Sigma^0 K_S^0$  combinations in Figs. 10, 11 and 12, respectively. In Fig. 7 there is a peak as expected from  $\Lambda_c^+(2285)$  and also some structure in the 1950–2150 MeV/ $c^2$  region that can be attributed to  $\Lambda_c^+$  decays with one or two missing pions. No other narrow peaks are evident.

In Fig. 8 the  $\Omega^-$  peak is prominent and there is a hint of a broad structure corresponding to the  $\Xi^-(1820)$ , but no other narrow structure is visible. In Fig. 9 we observe the  $\Xi_c^0(2472)$  at high momenta, and there are hints of the  $\Xi^0(1820)$ , but no other narrow structure. The  $\Sigma^0 K$  modes have much lower statistics, but show structure consistent with the corresponding

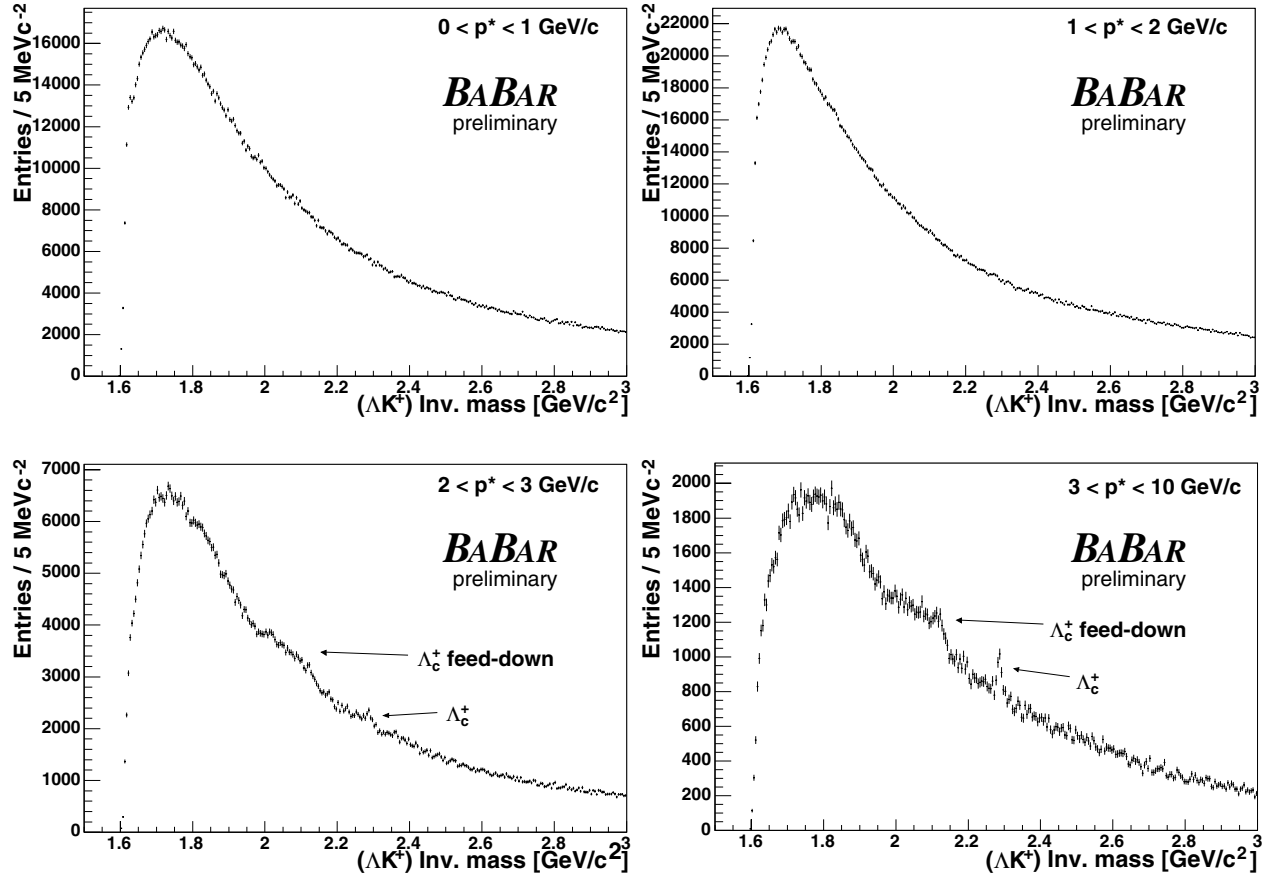


Figure 7: Invariant mass distributions of  $\Lambda^0 K^+$  for  $p^*$  in four different ranges.

$\Lambda^0 K$  mode. There is a hint of the  $\Xi^-(1950)$  at low  $p^*$  in the  $\Sigma^0 K^-$  mode. In no case is any unexpected narrow structure seen, and all evident structure is consistent with that due to known resonances. We have also examined the data in finer  $p^*$  bins and find no sign of a pentaquark signal in any  $p^*$  range.

We perform fits in ten  $p^*$  bins to the  $\Lambda^0 K^-$  and  $\Lambda^0 K_s^0$  mass distributions, in which we might expect signals near  $1860 \text{ MeV}/c^2$  from the  $\Xi_5^-$  and  $\Xi_5^0$  states, respectively. The resolution functions derived from the data and simulation are described by sums of two Gaussians with total rms of about  $4 \text{ MeV}/c^2$  that depend slightly on  $p^*$ . For each Breit-Wigner width we consider both 1 and 18  $\text{MeV}/c^2$ , as for the  $\Xi_5^{--}$ . The fits are performed over the mass range from  $1772 \text{ MeV}/c^2$  to  $1972 \text{ MeV}/c^2$  in order to exclude known resonances. The background function is a first-order polynomial.

We fix the masses to  $1862 \text{ MeV}/c^2$ , plus a shift obtained from the simulation in each  $p^*$  bin that does not exceed  $2 \text{ MeV}/c^2$ , and obtain the signal yields shown in Fig. 13. In all  $p^*$  bins the fit quality is good across the full mass range and the signal is consistent with zero. Systematic uncertainties on the fitting procedure are again found to be negligible compared with the statistical uncertainties, and variations of the mass and selection criteria give consistent results.

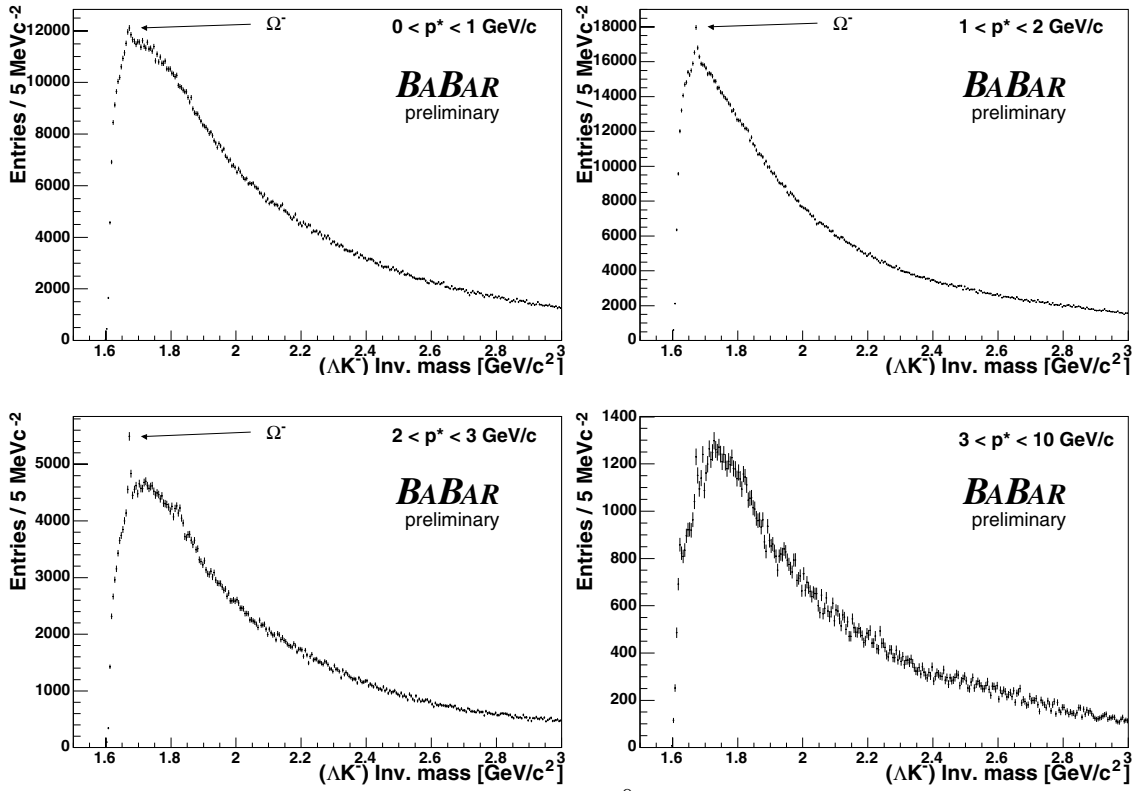


Figure 8: Invariant mass distributions of  $\Lambda^0 K^-$  for  $p^*$  in four different ranges.

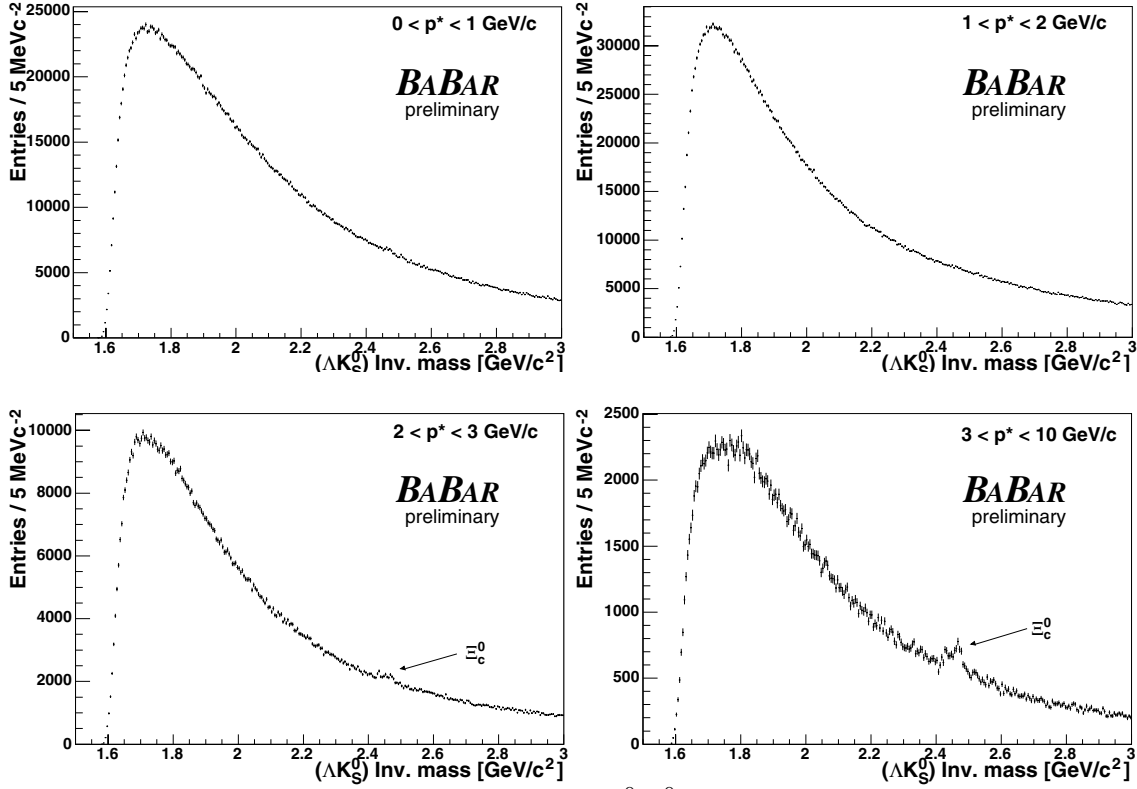


Figure 9: Invariant mass distributions of  $\Lambda^0 K_S^0$  for  $p^*$  in four different ranges.

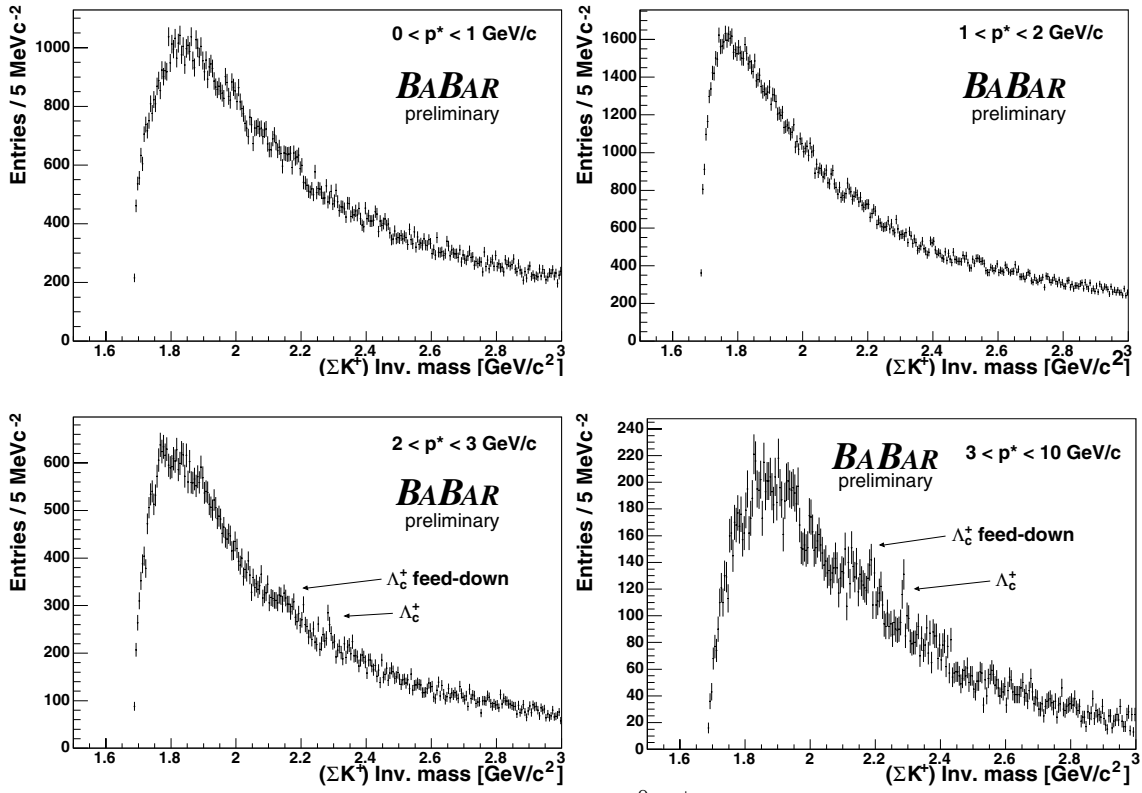


Figure 10: Invariant mass distributions of  $\Sigma^0 K^+$  for  $p^*$  in four different ranges.

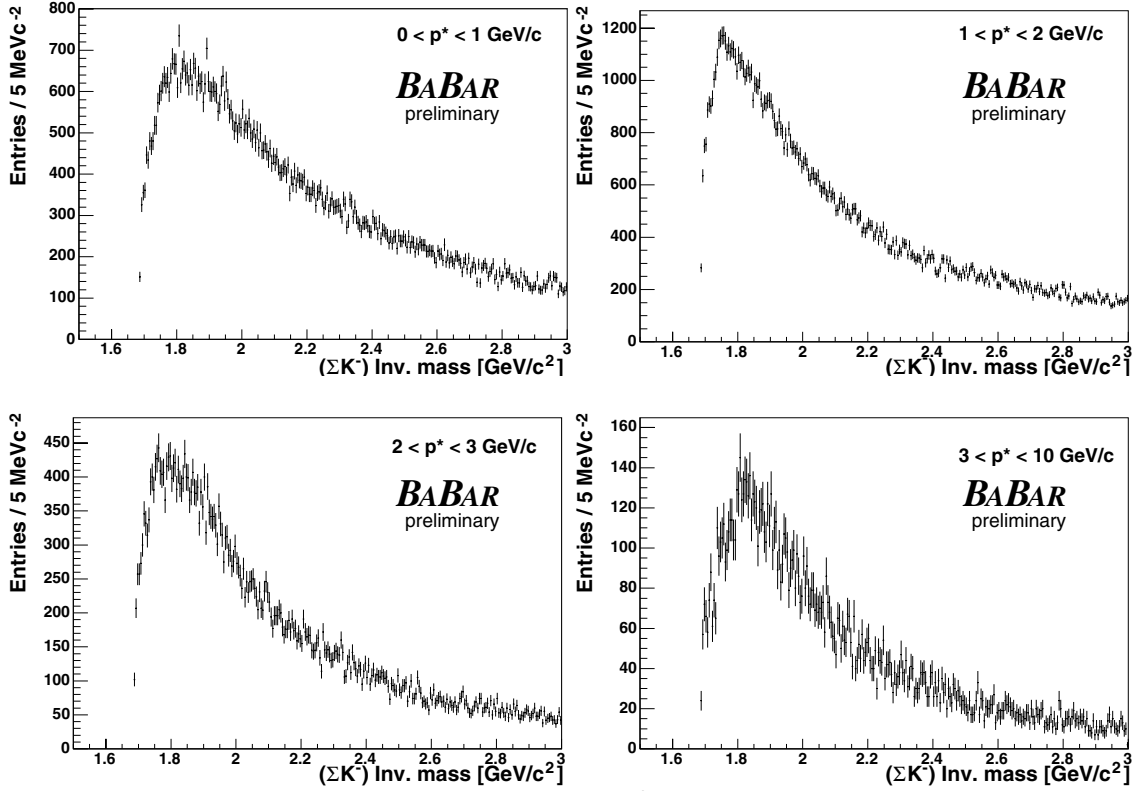


Figure 11: Invariant mass distributions of  $\Sigma^0 K^-$  for  $p^*$  in four different ranges.

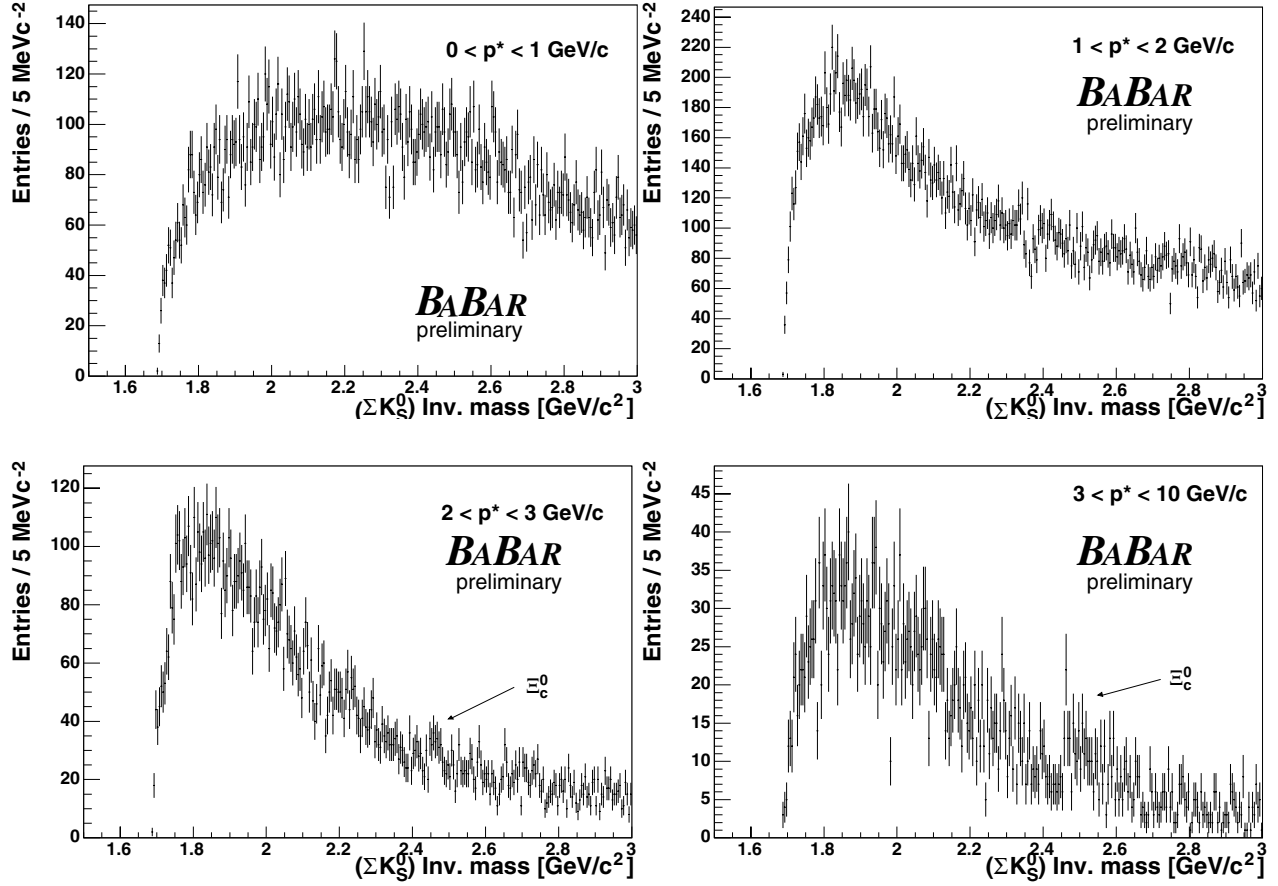


Figure 12: Invariant mass distributions of  $\Sigma^0 K_S^0$  for  $p^*$  in four different ranges.

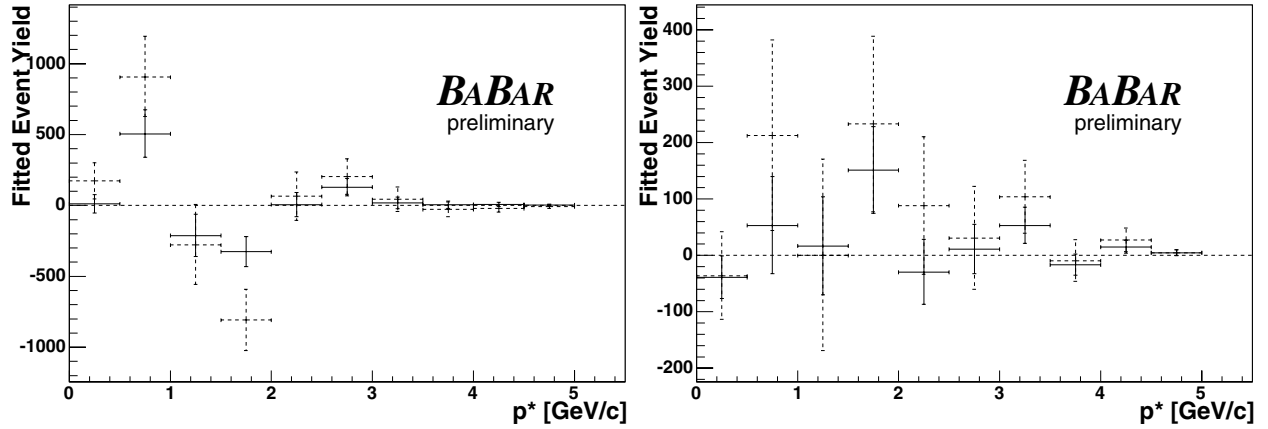


Figure 13: The  $\Xi_5^-$  (left) and  $\Xi_5^0$  (right) signal yields extracted from the fits to the  $\Lambda^0 K^-$  and  $\Lambda^0 K_S^0$  mass distributions, respectively, assuming a mass of  $1862 \text{ MeV}/c^2$  and width  $\Gamma = 1$  (solid) and  $\Gamma = 18 \text{ MeV}/c^2$  (dashed).

## 6 Upper Limits

For the states reported by previous experiments, there exist specific masses at which to search and experimental upper limits on the decay widths. We can therefore calculate upper limits on their differential production cross sections, with some assumptions on the branching fraction to the mode in which the search was made. We present such limits for the  $\Theta_5^+$ ,  $\Xi_5^{--}$ ,  $\Xi_5^-$  and  $\Xi_5^0$ .

For the  $\Theta_5^+(1540) \rightarrow pK_s^0$  we take the yields from the fits shown above (see Fig. 3) and convert them into cross sections by dividing by the efficiency (including the  $K_s^0 \rightarrow \pi^-\pi^+$  branching fraction), the integrated luminosity and the  $p^*$  bin width. The reconstruction efficiency is calculated from the simulation and corrected using data, and varies smoothly from 13% at low  $p^*$  to 22% at high  $p^*$ . It is checked by measuring the differential cross section for  $\Lambda_c^+ \rightarrow pK_s^0$  in the combination of  $q\bar{q}$  and  $\Upsilon(4S)$  events represented in our data, which is found to be consistent with the appropriate combination of previous measurements. If the  $\Theta_5^+$  is a  $udud\bar{s}$  pentaquark state, we expect only two possible decay modes,  $nK^+$  and  $pK^0$ , with very similar  $Q$  values and hence roughly equal branching fractions. Assuming half of the  $K^0$  appear as  $K_s^0$ , we arrive at a branching fraction  $B(\Theta_5^+ \rightarrow pK_s^0) = 1/4$ , and we divide by this value to obtain the total  $\Theta_5^+$  differential production cross section.

We then derive a conservative upper limit on this cross section in each bin. We consider only the physically allowed region, and scale the limit by a factor of  $(1 + \delta\epsilon/\epsilon)$ , where  $\delta\epsilon/\epsilon = 0.049$  is the sum in quadrature of the relative systematic uncertainties on the efficiency and luminosity. The relative luminosity uncertainty is 1%, and that on the efficiency is dominated by the 3.2% uncertainty on the reconstruction of pairs of tracks from a displaced vertex such as a  $K_s^0$ . The total is nearly independent of  $p^*$ .

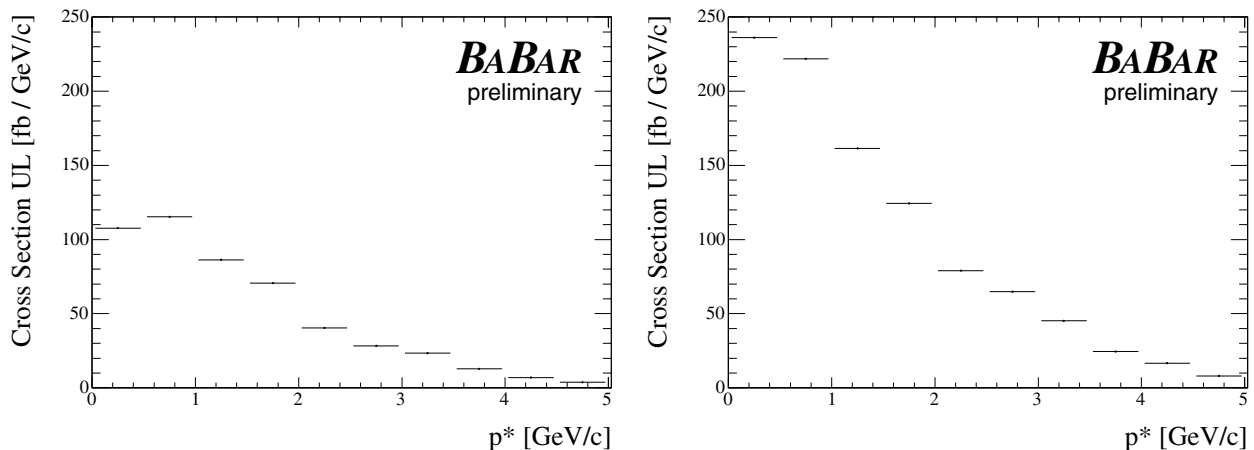


Figure 14: The 95% C.L. upper limit on the production cross-section for the  $\Theta_5^+$  assuming a mass of 1540  $\text{MeV}/c^2$  and a natural width  $\Gamma = 1 \text{ MeV}/c^2$  (left) or  $\Gamma = 8 \text{ MeV}/c^2$  (right), as a function of c.m. momentum  $p^*$ .

These upper limits are shown in Fig. 14 and tabulated in Table 2. Two sets of limits are shown; one corresponds to a very narrow state, and the other to a width at the current experimental upper limit of 8  $\text{MeV}/c^2$ . The limits correspond to the mass of 1540  $\text{MeV}/c^2$  used in the fits; repeating the analysis at several nearby mass values gives consistent limits.

The units are fb per GeV/c, and apply to the sum of all possible production processes. To isolate continuum and  $\Upsilon(4S)$  production we divide by the respective cross sections, and the corresponding limits on the numbers of pentaquarks per event are given in Table 2.

Similarly we convert the measured yields described above for the  $\Xi_5^{--}(1862) \rightarrow \Xi^-\pi^-$  (Fig. 6),  $\Xi_5^-(1862) \rightarrow \Lambda^0 K^-$  (Fig. 13) and  $\Xi_5^0(1862) \rightarrow \Lambda^0 K_s^0$  (Fig. 13) decays into cross sections. Here we assume a mass of 1862 MeV/c<sup>2</sup> and present limits for both a very narrow hypothesis and for  $\Gamma = 18$  MeV/c<sup>2</sup>. The  $\Xi_5^{--}(1862) \rightarrow \Xi^-\pi^-$  reconstruction efficiency varies smoothly from 6.5% at low  $p^*$  to 12% at high  $p^*$ , and has been checked using the observed  $\Xi^{*0}(1530) \rightarrow \Xi^-\pi^+$  signal. Its relative systematic uncertainty again varies slightly with  $p^*$ , and its average value of  $\delta\epsilon/\epsilon = 0.064$  is larger than for the  $pK_s^0$  mode, as there are two displaced vertices and more tracks in the decay. The  $\Xi_5^-(1862) \rightarrow \Lambda^0 K^-$  efficiency varies from 10% at low  $p^*$  to 27% at high  $p^*$ , is checked with the  $\Omega^- \rightarrow \Lambda^0 K^-$  signal, and the average  $\delta\epsilon/\epsilon = 0.052$  is similar to the  $pK_s^0$  mode. The  $\Xi_5^0(1862) \rightarrow \Lambda^0 K_s^0$  efficiency varies from 3.5% at low  $p^*$  to 13% at high  $p^*$ , and  $\delta\epsilon/\epsilon = 0.072$  is similar to the  $\Xi^-\pi^-$  mode.

We assume a  $\Xi_5^{--} \rightarrow \Xi^-\pi^-$  branching fraction of one-half; for the  $\Xi_5^-$  and  $\Xi_5^0$  we do not assume branching fractions into the measured modes, but present limits on the product of the production cross section and branching fraction. Again the results are independent of the assumed mass; they are shown in Figs. 15 and 16, and tabulated in Tables 3, 4 and 5.

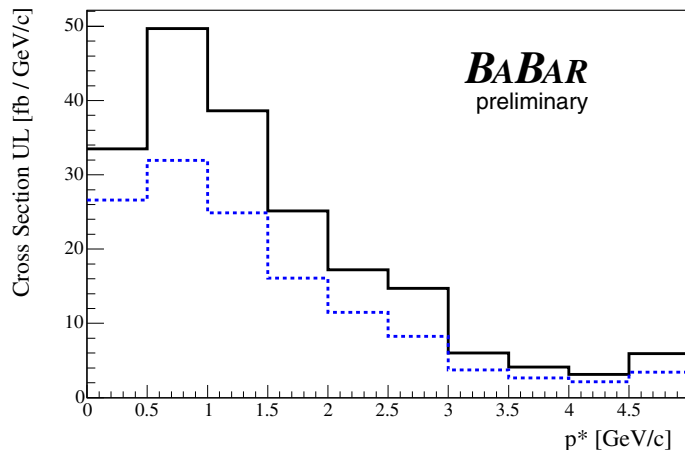


Figure 15: The 95% C.L. upper limit on the production cross-section for  $\Xi_5^{--}$  assuming a natural width of  $\Gamma = 1$  (dashed) and  $\Gamma = 18$  MeV/c<sup>2</sup> (solid), as a function of c.m. momentum  $p^*$ .

In order to quote limits on the total production cross section (times branching fraction) we must either know the momentum spectrum or believe that it does not vary rapidly on the scale of our bin size. Since the latter is true in the simulation, we assign conservative, model-independent upper limits on the total numbers of pentaquarks produced per  $e^+e^- \rightarrow q\bar{q}$  event ( $\Upsilon(4S)$  decay) by summing each differential cross section over the  $p^*$  range from zero to the kinematic limit for 5.3 GeV jets ( $B$  meson decays), taking into account the fact that most of the systematic error is common to all bins. Limits are derived from these sums by the same method as in each bin, and are listed in Tables 2–5. Any postulated spectrum can be folded with our differential limit to obtain a limit on the total cross section assuming that spectrum, which will be lower than the model independent limits given in the tables.

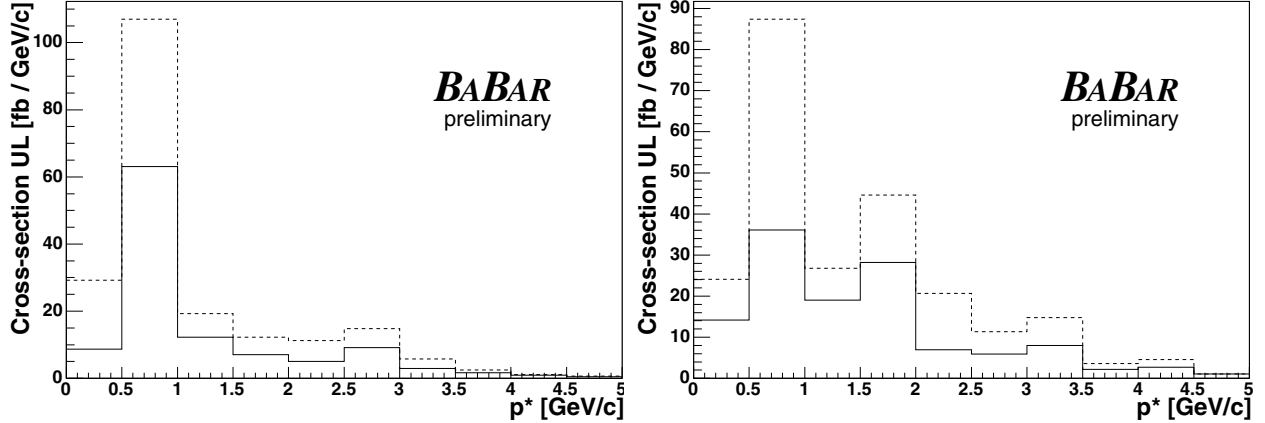


Figure 16: The 95% C.L. upper limits on the production cross-section for  $\Xi_5^-$  times its branching fraction into  $\Lambda^0 K^-$  (left), and  $\Xi_5^0$  times its branching fraction into  $\Lambda^0 K_S^0$  (right), assuming a natural width of  $\Gamma = 1 \text{ MeV}/c^2$  (solid) and  $\Gamma = 18 \text{ MeV}/c^2$  (dashed), as a function of c.m. momentum  $p^*$ .

## 7 Summary

We have performed a preliminary high statistics search for the reported states  $\Theta_5^+$  (1540),  $\Xi_5^{--}$  (1862),  $\Xi_5^-$  (1862) and  $\Xi_5^0$  (1862) in  $e^+e^-$  annihilations, and also for most of the other members of the pentaquark octet and anti-decuplet to which they are postulated to belong. In all cases we observe clear signals for known baryon resonances that demonstrate sensitivity to any new narrow resonances, with invariant mass resolution better than the reported upper limits on the widths of the respective states. We find no evidence for the production of such states in  $123 \text{ fb}^{-1}$  of *BABAR* data. For the reported states, we see no excess at the measured invariant mass values and use the reported limits on their widths to set upper limits on their inclusive production in our search modes in both  $e^+e^- \rightarrow q\bar{q}$  events and  $\Upsilon(4S)$  decays. These limits are at the level of  $10^{-4}$ – $10^{-5}$  per event, depending on the width assumed, and are valid for any narrow state in the vicinity of 1540 or 1860  $\text{MeV}/c^2$ . The searches for other members of the multiplets show no evidence for an unknown narrow resonance at any mass between threshold for the decay mode used and the kinematic limit.

In order to limit the production rates we must know the branching fraction of each state into the decay mode used in the search. In the case of the  $\Theta_5^+$ , we take this to be 1/4, as noted above. For  $\Xi_5^{--}$  a similar argument that  $\Xi^- \pi^-$  and  $\Sigma^- K^-$  dominate and have roughly equal branching fractions leads to a branching fraction of 1/2. Taking the upper limit widths, we calculate 95% C.L. upper limits on the total production rates of  $1.1 \times 10^{-4}$   $\Theta_5^+$  and  $1.0 \times 10^{-5}$   $\Xi_5^{--}$  per  $e^+e^- \rightarrow q\bar{q}$  event (preliminary); these are roughly a factor of eight and four below the typical values measured for ordinary octet and decuplet baryons of the same masses of  $8 \times 10^{-4}$  and  $4 \times 10^{-5}$ , respectively, as illustrated in Fig. 17.

The situation is more complex for the  $\Xi_5^-$  and  $\Xi_5^0$  as the mixing between the members of the anti-decuplet and the octet is unknown. In these two cases the branching fraction of an antidecuplet state of mass  $\sim 1860 \text{ MeV}/c^2$  to the measured mode could be anywhere from zero to  $\sim 1/3$ . The best limit that could be set, assuming the value of 1/3, would therefore be roughly  $15 \times 10^{-5}$   $\Xi_5^-$  or  $\Xi_5^0$  per  $e^+e^- \rightarrow q\bar{q}$  event, which is well above the “expected” value

Table 2: The measured  $\Theta_5^+$  signal yield in each  $p^*$  bin, assuming a mass of 1540 MeV/ $c^2$  and two values of the natural width  $\Gamma$  in MeV/ $c^2$ . The corresponding upper limits at the 95% C.L. on the  $\Theta_5^+$  differential production cross section, the number of  $\Theta_5^+$  produced per  $e^+e^- \rightarrow q\bar{q}$  event and the number per  $\Upsilon(4S)$  decay.

$\Theta_5^+(1540)$ (preliminary)								
$p^*$ Range (GeV/ $c$ )	Yield ( $pK_s^0$ mode)		X-section U.L. (fb/GeV $c^{-1}$ )		$q\bar{q}$ event U.L. ( $10^{-5}/(\text{evt}\cdot\text{GeV}c^{-1})$ )		$\Upsilon(4S)$ decay U.L. ( $10^{-5}/(\text{evt}\cdot\text{GeV}c^{-1})$ )	
	$\Gamma = 1$	$\Gamma = 8$	$\Gamma = 1$	$\Gamma = 8$	$\Gamma = 1$	$\Gamma = 8$	$\Gamma = 1$	$\Gamma = 8$
0.0–0.5	$107 \pm_{134}^{139}$	$288 \pm_{242}^{283}$	107.6	236.2	3.17	6.97	10.76	23.62
0.5–1.0	$-178 \pm_{236}^{238}$	$-194 \pm_{452}^{457}$	115.3	221.8	3.40	6.54	11.53	22.18
1.0–1.5	$19 \pm_{208}^{210}$	$-31 \pm_{410}^{406}$	86.2	161.5	2.54	4.76	8.61	16.14
1.5–2.0	$109 \pm_{156}^{156}$	$112 \pm_{310}^{307}$	70.7	124.4	2.09	3.67	7.07	12.44
2.0–2.5	$-158 \pm_{113}^{114}$	$-322 \pm_{243}^{222}$	40.4	79.0	1.19	2.33	2.83	7.90
2.5–3.0	$-38 \pm_{83}^{83}$	$41 \pm_{164}^{175}$	28.3	64.8	0.83	1.91	2.35	6.48
3.0–3.5	$33 \pm_{59}^{59}$	$50 \pm_{117}^{119}$	23.4	45.2	0.69	1.33	—	—
3.5–4.0	$-11 \pm_{39}^{39}$	$-56 \pm_{80}^{74}$	12.9	24.5	0.38	7.23	—	—
4.0–4.5	$4 \pm_{21}^{22}$	$25 \pm_{44}^{47}$	6.8	16.6	0.20	4.88	—	—
4.5–5.0	$1 \pm_{12}^{12}$	$6 \pm_{24}^{24}$	3.7	7.9	0.11	2.33	—	—
Total	—	—	182.8	363.1	5.39	10.71	17.90	34.98
			(fb)		( $10^{-5}/\text{event}$ )		( $10^{-5}/\text{event}$ )	

of  $4 \times 10^{-5}$ . The study of additional modes is needed to elucidate the production properties of these states.

## Acknowledgements

We are grateful for the extraordinary contributions of our PEP-II colleagues in achieving the excellent luminosity and machine conditions that have made this work possible. The success of this project also relies critically on the expertise and dedication of the computing organizations that support *BABAR*. The collaborating institutions wish to thank SLAC for its support and the kind hospitality extended to them. This work is supported by the US Department of Energy and National Science Foundation, the Natural Sciences and Engineering Research Council (Canada), Institute of High Energy Physics (China), the Commissariat à l’Energie Atomique and Institut National de Physique Nucléaire et de Physique des Particules (France), the Bundesministerium für Bildung und Forschung and Deutsche Forschungsgemeinschaft (Germany), the Istituto Nazionale di Fisica Nucleare (Italy), the Foundation for Fundamental Research on Matter (The Netherlands), the Research Council of Norway, the Ministry of Science and Technology of the Russian Federation, and the Particle Physics and Astronomy Research Council (United Kingdom). Individuals have received support from CONACyT (Mexico), the A. P. Sloan Foundation, the Research Corporation, and the Alexander von Humboldt Foundation.

Table 3: The measured  $\Xi_5^{--}$  signal yield in each  $p^*$  bin, assuming a mass of 1862 MeV/ $c^2$  and two values of the natural width in MeV/ $c^2$ . The corresponding upper limits at the 95% C.L. on the  $\Xi_5^{--}$  differential production cross section, the number of  $\Xi_5^{--}$  produced per  $e^+e^- \rightarrow q\bar{q}$  event and the number per  $\Upsilon(4S)$  decay.

$\Xi_5^{--} \rightarrow \Xi^- \pi^-$ (preliminary)								
$p^*$ Range (GeV/ $c$ )	Yield		X-section U.L. (fb/GeV $c^{-1}$ )		$q\bar{q}$ event U.L. ( $10^{-5}/(\text{evt}\cdot\text{GeV}c^{-1})$ )		$\Upsilon(4S)$ decay U.L. ( $10^{-5}/(\text{evt}\cdot\text{GeV}c^{-1})$ )	
	$\Gamma = 1$	$\Gamma = 18$	$\Gamma = 1$	$\Gamma = 18$	$\Gamma = 1$	$\Gamma = 18$	$\Gamma = 1$	$\Gamma = 18$
0.0–0.5	13±26	−7±37	26.6	33.5	0.78	0.99	2.53	3.19
0.5–1.0	−62±52	−128±67	31.9	49.7	0.94	1.46	3.04	4.73
1.0–1.5	−56±50	−63±76	24.9	38.6	0.73	1.14	2.37	3.68
1.5–2.0	−70±52	−102±62	16.1	25.1	0.47	0.74	1.53	2.39
2.0–2.5	−48±33	−64±50	11.5	17.2	0.34	0.51	1.09	1.64
2.5–3.0	5±28	21±35	8.3	14.7	0.24	0.43	0.79	1.40
3.0–3.5	−25±15	−36±28	3.7	6.0	0.11	0.18	—	—
3.5–4.0	5±10	8±12	2.6	4.1	0.08	0.12	—	—
4.0–4.5	3±10	2±11	2.1	3.1	0.06	0.09	—	—
4.5–5.0	1±12	1±22	3.4	5.9	0.10	0.17	—	—
Total	—	—	22.0	33.7	0.65	0.99	2.11	3.20
			(fb)		$(10^{-5}/\text{event})$		$(10^{-5}/\text{event})$	

Table 4: The measured  $\Xi_5^-$  signal yield in each  $p^*$  bin, assuming a mass of 1862 MeV/ $c^2$  and two values of the natural width in MeV/ $c^2$ . The corresponding upper limits at the 95% C.L. on the  $\Xi_5^-$  differential production cross section times its branching fraction  $B$  into  $\Lambda^0 K^-$ ,  $B \times$  the number of  $\Xi_5^-$  produced per  $e^+e^- \rightarrow q\bar{q}$  event and  $B \times$  the number per  $\Upsilon(4S)$  decay.

$\Xi_5^- \rightarrow \Lambda^0 K^-$ (preliminary)								
hline $p^*$ Range (GeV/ $c$ )	Yield		X-section U.L. (fb/ GeV $c^{-1}$ )		$q\bar{q}$ event U.L. ( $10^{-5}/(\text{evt}\cdot\text{GeV}c^{-1})$ )		$\Upsilon(4S)$ decay U.L. ( $10^{-5}/(\text{evt}\cdot\text{GeV}c^{-1})$ )	
	$\Gamma = 1$	$\Gamma = 18$	$\Gamma = 1$	$\Gamma = 18$	$\Gamma = 1$	$\Gamma = 18$	$\Gamma = 1$	$\Gamma = 18$
0.0–0.5	11± <sup>65</sup> <sub>64</sub>	174± <sup>128</sup> <sub>127</sub>	40.9	122.4	1.21	3.61	3.90	11.66
0.5–1.0	505± <sup>171</sup> <sub>164</sub>	906± <sup>287</sup> <sub>277</sub>	220.9	385.7	6.52	11.38	21.04	36.73
1.0–1.5	−213± <sup>151</sup> <sub>148</sub>	−278± <sup>285</sup> <sub>278</sub>	62.8	118.8	1.85	3.50	5.98	11.31
1.5–2.0	−326± <sup>106</sup> <sub>105</sub>	−808± <sup>216</sup> <sub>215</sub>	34.3	69.8	1.01	2.06	3.27	6.65
2.0–2.5	6± <sup>85</sup> <sub>84</sub>	65± <sup>172</sup> <sub>170</sub>	24.7	57.2	0.73	1.69	2.35	5.45
2.5–3.0	129± <sup>62</sup> <sub>61</sub>	203± <sup>126</sup> <sub>125</sub>	33.0	59.5	0.97	1.76	—	—
3.0–3.5	17± <sup>42</sup> <sub>41</sub>	43± <sup>87</sup> <sub>86</sub>	12.8	27.5	0.38	0.81	—	—
3.5–4.0	4± <sup>26</sup> <sub>26</sub>	−28± <sup>53</sup> <sub>52</sub>	7.5	13.8	0.22	0.41	—	—
4.0–4.5	7± <sup>15</sup> <sub>14</sub>	−21± <sup>28</sup> <sub>27</sub>	3.9	6.0	0.12	0.18	—	—
4.5–5.0	3± <sup>6</sup> <sub>5</sub>	−8± <sup>13</sup> <sub>12</sub>	1.9	3.3	0.06	0.10	—	—
Total	—	—	83.6	181.0	2.76	5.34	7.87	15.88
			(fb)		$(10^{-5}/\text{event})$		$(10^{-5}/\text{event})$	

Table 5: The measured  $\Xi_5^0$  signal yield in each  $p^*$  bin, assuming a mass of 1862 MeV/ $c^2$  and two values of the natural width in MeV/ $c^2$ . The corresponding upper limits at the 95% C.L. on the  $\Xi_5^0$  differential production cross section times its branching fraction  $B$  into  $\Lambda^0 K_s^0$ ,  $B \times$  the number of  $\Xi_5^0$  produced per  $e^+e^- \rightarrow q\bar{q}$  event and  $B \times$  the number per  $\Upsilon(4S)$  decay.

$\Xi_5^0 \rightarrow \Lambda^0 K_s^0$ (preliminary)								
$p^*$ Range (GeV/ $c$ )	Yield		X-section U.L. (fb/GeV $c^{-1}$ )		$q\bar{q}$ event U.L. ( $10^{-5}/(\text{evt}\cdot\text{GeV}c^{-1})$ )		$\Upsilon(4S)$ decay U.L. ( $10^{-5}/(\text{evt}\cdot\text{GeV}c^{-1})$ )	
	$\Gamma = 1$	$\Gamma = 18$	$\Gamma = 1$	$\Gamma = 18$	$\Gamma = 1$	$\Gamma = 18$	$\Gamma = 1$	$\Gamma = 18$
0.0–0.5	$-39 \pm_{38}^{38}$	$-36 \pm_{77}^{78}$	46.7	95.8	1.38	2.83	4.45	9.12
0.5–1.0	$53 \pm_{85}^{87}$	$212 \pm_{168}^{169}$	105.7	256.4	3.12	7.56	10.07	24.42
1.0–1.5	$17 \pm_{87}^{87}$	$0 \pm_{169}^{171}$	60.6	108.5	1.79	3.20	5.77	10.34
1.5–2.0	$151 \pm_{76}^{78}$	$233 \pm_{156}^{155}$	71.0	126.2	2.09	3.72	6.76	12.02
2.0–2.5	$-30 \pm_{57}^{58}$	$88 \pm_{122}^{122}$	23.0	65.3	0.68	1.93	2.19	6.22
2.5–3.0	$11 \pm_{43}^{44}$	$31 \pm_{91}^{92}$	18.1	39.1	0.54	1.15	—	—
3.0–3.5	$53 \pm_{32}^{32}$	$104 \pm_{64}^{65}$	20.3	40.2	0.60	1.19	—	—
3.5–4.0	$-17 \pm_{19}^{19}$	$-9 \pm_{36}^{37}$	6.8	13.2	0.20	0.39	—	—
4.0–4.5	$15 \pm_{11}^{12}$	$27 \pm_{21}^{21}$	6.9	12.6	0.20	0.37	—	—
4.5–5.0	$5 \pm_{5}^6$	$5 \pm_{5}^6$	2.7	2.7	0.08	0.08	—	—
Total	—	—	82.8	204.7	2.44	6.04	7.25	18.02
			(fb)		( $10^{-5}/\text{event}$ )		( $10^{-5}/\text{event}$ )	

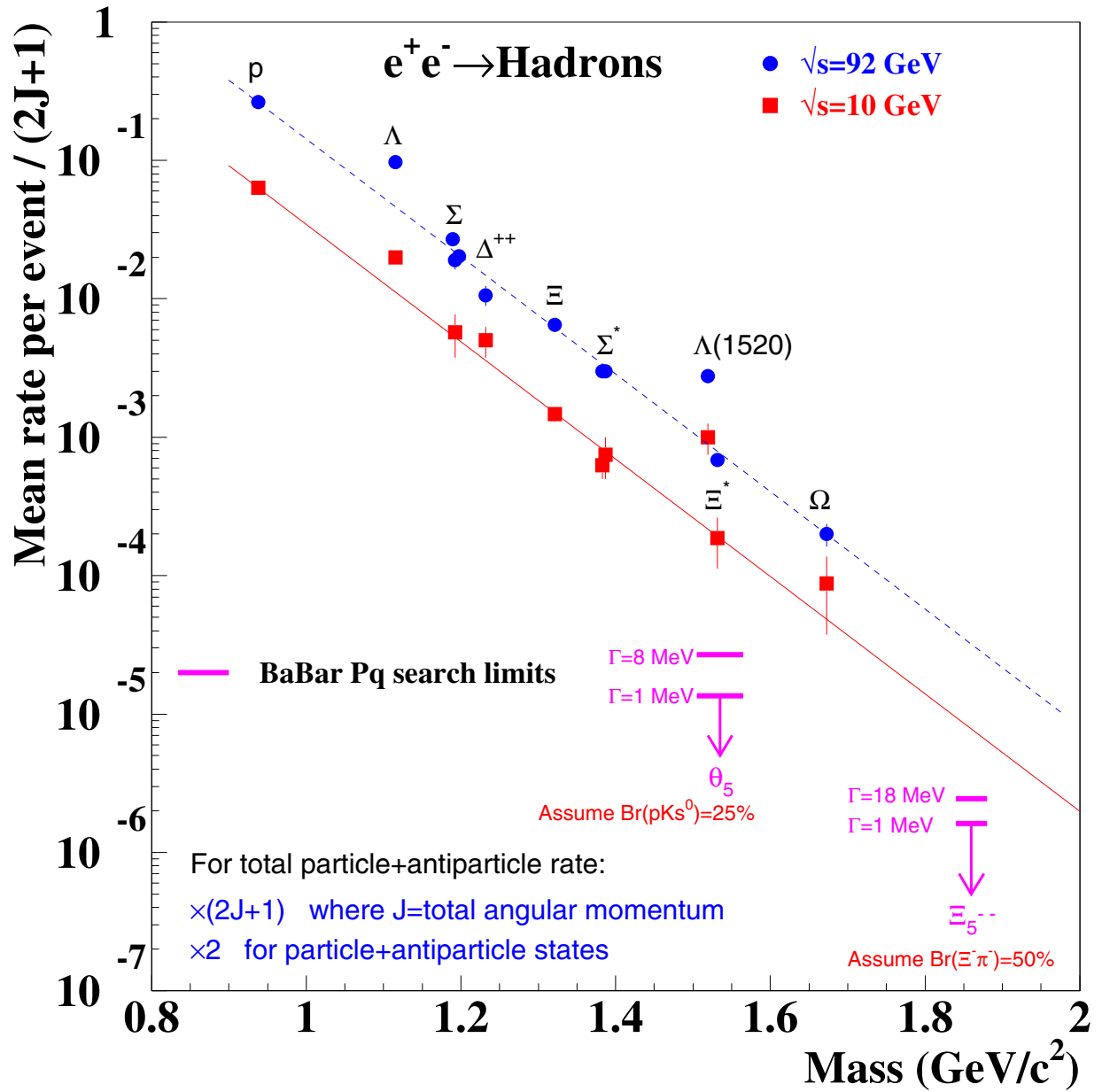


Figure 17: Compilation of baryon production rates in  $e^+e^-$  annihilation [15] from experiments at the  $Z^0$  (circles) and  $\sqrt{s} \approx 10 \text{ GeV}$  (squares) as a function of baryon mass. The vertical scale accounts for the number of spin and particle+antiparticle states, and the lines are chosen to guide the eye. The arrows indicate our preliminary upper limits on spin-1/2  $\Theta_5^+$  and  $\Xi_5^{--}$  pentaquark states, assuming the branching fractions shown, and are seen to lie below the solid line.

## References

- [1] LEPS Collaboration, T. Nakano *et al.*, Phys. Rev. Lett. **91**, 012002 (2003).
- [2] SAPHIR Collaboration, J. Barth *et al.*, Phys. Lett. **B 572**, 127 (2003).
- [3] CLAS Collaboration, V. Kubarovsky *et al.*, Phys. Rev. Lett. **92**, 032001 (2004). Erratum; *ibid*, 049902.
- [4] DIANA Collaboration, V.V. Barmin *et al.*, Phys. Atom. Nucl. **66**, 1715 (2003).
- [5] SVD Collaboration, A. Aleev *et al.*, hep-ex/0401024 (2004).
- [6] HERMES Collaboration, A. Airapetian *et al.*, Phys. Lett. **B 585**, 213 (2004).
- [7] COSY-TOF Collaboration, M. Abdel-Bary *et al.*, Phys. Lett. **B 595**, 127 (2004).
- [8] NA49 Collaboration, C. Alt *et al.*, Phys. Rev. Lett. **92**, 042003 (2004).
- [9] H1 Collaboration, A. Aktas *et al.*, hep-ex/0403017 (2004).
- [10] See, e.g., J. Pochodzalla, hep-ex/0406077 (2004) and references therein.
- [11] D. Diakonov, V. Petrov and M.V. Polyakov, Z. Phys. **A 359**, 305 (1997).
- [12] M. Karliner and H. Lipkin, hep-ph/0402260 (2004).
- [13] R. Jaffe and F. Wilczek, Phys. Rev. Lett. **91**, 232003 (2003).
- [14] The *BABAR* Collaboration, B. Aubert *et al.*, Nucl. Instrum. Methods **A 479**, 1 (2002).
- [15] Particle Data Group, K. Hagiwara *et al.*, Phys. Rev. **D 66**, 010001 (2002).
- [16] T. Sjostrand, Comput. Phys. Commun. **82**, 74 (1994).